REPORT TO JOINT INDUSTRY
ULSLEA PROJECT SPONSORS

LOADING AND CAPACITY CHARACTERISTICS OF

PILE FOUNDATIONS

Correlation of Calculation Results with ULSLEA

by
Zhaohui Jin
and
Professor Robert Bea

Marine Technology &Management Group
Department of Civil & Environmental Engineering
UNIVERSITY OF CALIFORNIA AT BERKELEY

January, 1998

I

TABLE OF CONTENTS

Part   **Page No.**

Chapter 1

Introduction

1.1   Background

In the field of Offshore Engineering, foundation is always an essential element for fixed platforms. In the Gulf of Mexico, most fixed platforms are pile-supported. The response of the pile foundations of these platforms to the external loading, both dynamic and static, are a classical subject for offshore engineers. With the extension of offshore operations into deeper water and more hostile environments, concerns with implications of foundation design on overall platform costs, and the need to incorporate more realistic foundation response characterizations into the requalification analyses of existing structures have brought a recent focus on the dynamic response of marine foundations. The general engineering guidelines for treatment of such problems are still under . development and subject to update. The needs for high quality experimental and analytical research are highlighted. Pile foundations are the key components for the whole drilling and production systems, which determine the safety, serviceability, durability and compatibility of such systems. It is desired that the pile foundations are designed in a safe and economic manner.

An study was performed by the Marine Technology and Management Group at the University of California at Berkeley in 1997, parallel to the joint industry ULSLEA project. This study has an emphasis on the dynamic response of a single pile, especially for the ultimate state. The pile's response and capacities are calculated by different computer models. As the output of this effort, the calculation results by these different methods are correlated with those obtained by ULSLEA.

1.2 Objectives of this Report

A lot of detailed research has been done with respect to pile response in this The work performed include:

- Extending SPASM computer code used in previous study (Jin and Bea, August, 1997) to the non-linear pile behavior after first yielding occurs, obtaining an estimation of the ultimate capacity of a single pile to lateral loading.

- Developing an analysis model which is capable of handling both the nonlinear piles and nonlinear-hysteretic soil resistance, with proper supporting computer codes, such as Drain3D.

- With the developed model, performing analysis of the pile's behaviors beyond the elastic range up to final collapse.

- Using the analysis model ULSLEA, predict the ultimate capacity of a single pile by a simplified approach.

- Correlating the pile capacity predictions obtained by the different analysis models above to estimate the bias and uncertainties from the prediction methods.

The purpose of this report is to summarize the results of the detailed complex pile response analysis and correlate them with the results from the ULSLEA program. Excellent agreements are obtained between the detailed complex analysis tools and ULSLEA programs. By comparing the calculation results from different methods, this report demonstrated the validity of the simplified ULSLEA. These results provide the information on the bias of the ultimate capacities that ULSLEA can develop compared with the API guideline and the detailed numerical simulation method such as Drain3D model.

1.3   Organization of the Report

This report is divided into 5 parts. Chapter 1 is the background and objectives of the report. Chapter 2 gives a review of the current research in this field; describes the basic assumption and approach in this study; details the building-up process of the analysis models in this study, with an emphasis on the new DRAIN3D numerical model. Chapter 3 is about the lateral response of a single pile, including the first yielding capacity, ultimate capacity. The analysis addresses pile-soil systems behaviors under static loading, cyclic loading and fast loading. The lateral responses were predicted by SPASM, DRAIN3D, ULSLEA3.0 and ULSLEA phase IV. Chapter 4 summarizes the analysis of the axial response of a single pile. The basic approach is the same as that for lateral response. The behaviors under static, fast and cyclic loading are studied. The calculating code is DRAIN3D and UlSLEA3.0. A calculation is also performed according to the API RP2A guideline.   Chapter 5 is the conclusions and recommendations.
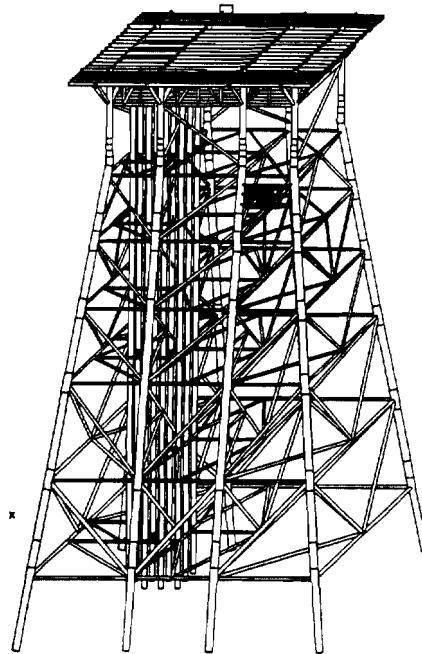
Fig. 1.1 Typical pile supported platform

Chapter 2

Approach and Description
of the Analysis Models

2.1   Current Research

The performance (load-deformation) characteristics of pile foundations is a classical research subject in the design and construction of offshore oil drilling platforms. Realistic modeling of pile foundation is crucial to the validity of the results of static and dynamic structural analyses of offshore platforms. Furthermore, the comprehension of both the static and dynamic response of a single pile to the external loading is the corner stone for all the analyses in this field. The state-of-art design technique and theory concerning pile foundation are still under development, though there have been extensive research effort on this topic. In the past design and construction practice, too often have foundation failures been predicted to be the dominant failure mode of platforms, seldom have the observed failure modes included failure of foundation elements. This fact indicates that the traditional methods of predicting the ultimate capacity of pile foundations are in general conservatively biased.

The state-of-practice design criteria of pile foundation have a static or pseudo-static approach. This kind of calculation method is widely used. To keep the analysis tractable in interpreting of complicated pile-soil interaction phenomenon, this kind of method has several simplifying assumptions:

- The capacities of offshore piles can be calculated using methods based primarily upon tests of relatively short onshore piles that were loaded slowly to failure, i.e. the validity of the method are usually correlated to the static loading test;

- Pile capacity reductions due to the degradation of soil resistance by cyclically applied loading do not need to be considered explicitly; and

- Pile capacity increases that can occur in clay soils during rapid loading also do not need to be considered explicitly.

This static pile-capacity method has been used to determine the pile foundation configuration for the pile foundations of the more than 6,000 offshore platforms that are now located on the world's continental shelves. These foundations have had a remarkably good record of reliability. This has proved the validity of the current design criteria. The American Petroleum Institute (API) has developed such guidelines for evaluation of the capacity of the pile foundations (API RP2A, 20th edition 1993). These guidelines address a wide scope of topics such as operating and environmental loading; determination of static capacity; influences on capacity, stiffness; applications of discrete element and continuum analytical models; use of in situ and laboratory soil test and prototype pile-load tests in soil characterizations; evaluation of load, resistance, and deformation characterizations at serviceability and ultimate limit states; and interpretations and applications of results. These guidelines represent the culmination of a 20-year development effort of worldwide research regarding pile foundation performance.

However, as stated in the principal assumption of the static-capacity calculation method, two important factors, which affects the in-situ performance of pile foundations are not addressed: the loss of strength and stiffness of the pile-soil system due to cyclic loading, which is obvious in the wave loading during a hurricane; and the increase of strength and stiffness due to the high loading rate effects, which is typical in an earthquake. Bea (1984) summarized the trends that have been observed for piles tested for these two effects. Load rate effects can result in effective increases in pile strength and stiffness on the order of 20% to 80% or more for loading rates consistent with wave action. Assuming the trend continues without degradation, the expected increases for earthquake loading rates would be much higher, shall be to the order of 2-3. Cyclic

loading tends to result in progressive deterioration of pile foundation strength and stiffness. Hysteresis curves generated for piles will tend to exhibit pinching and softening for repeated cycles. Tests have shown that the soil support for the pile in the top stratums will suffer a drastic reduction due to cyclic loading from wave force. How to reflect these two effects in the prediction of the real in-situ pile foundation response is still under investigation. For the sake of conservation, current state-of-the-practice in offshore engineering tends to recognize cyclic degradation in determining response. This is achieved by implicitly incorporating these effects into the static capacity analysis, or by including such negative effects in the safety index in pile foundation design. Meanwhile, the beneficial loading rate effects are not taken into account. It is obvious that further research is needed in this area to better define the interaction between these two phenomena.

Assessing the structural integrity of an offshore platform requires balance between considerations of capacity and economic. In the case of foundations, this requirement translates into the need of better understanding of their performance and more realistic modeling of their behavior so that the foundations are not designed with unnecessary reserve capacity. This need has led to focus on the study of dynamic response of pile foundations. This analysis incorporates the two major factors not addressed by static method. It also involves other important factors affecting the real dynamic response of the pile foundations. This effort has resulted in numerous valuable information in guiding the design and construction.

Bea (1984) published a key note paper on the dynamic response of the pile foundation. It provides a summary of the basic approaches to the investigation of this problem. The main concerns in the prediction of the pile foundation behaviors are as follows:

- Dynamic response depends primarily on external loading patterns and the inherent structure properties;

- Environmental loadings are dynamic. Loadings on platforms are developed from the motionless ocean and earth crust. It is crucial that they are well understood;

- Non-linearity is a key concern in the analysis: in presence of soil, which are highly nonlinear, the pile foundation exhibits complicated coupling action between the soil and the steel piles;

- High strain rates increase strength and stiffness;

- Cyclic strains decrease strength and stiffness;

- Cyclic loading leads to accumulated displacements;

- Damping developed from pile foundation is important;

2.2   Uncertainties in the Pile response prediction

In practice, designers of offshore platforms and pile foundations deal with numerous uncertainties, including imperfect knowledge of the frontier such as: the loads to which the superstructure is subjected; the behavior of the superstructure under those loads; and how the founding soils respond when those loads are transmitted to them via the foundation piles.

In the frontiers mentioned above, Tang(1988, 1990), Bea(1983),Folse(1989), Ruiz(1984, 1986), Yegian and Hadley(1979) , Olson(1984), Kullhawy(1984), Briaud and Tucker(1986) have identified various factors affecting offshore pile capacity prediction. These studies suggested estimation of the calculation bias the uncertainty statistics properties associated with these factors. The conclusions concerning the major component of uncertainties involved in the prediction of pile capacity can be summarized as follows:

- Soil properties uncertainties;
- Load parameters uncertainties;
- Prediction model error;

Uncertainties in the soil properties are a major contribution to the overall system uncertainties. There are several very important soil parameters needed to define the p-y and t-z curves for pile foundation analysis, such as undrained shear strength, unit weight, friction angle, and shear modulus. As an inherent character of soil mechanics, these parameters subject to large variation due to natural inhomogeneous properties of in-situ soils, and distribution during lab or in-situ test, not to mention the system variation derived from various test methods. The major uncertainty sources in soil parameters are listed as follows:

- **Non-standard sampling or test methods**

  Their effects are not completely avoidable on the determination of the soil properties, even though very high quality test are performed.

- **Spatial variation of soil properties**

  This variation is due to the randomness associated with the natural deposition process, which is the inherent variability with the macro geological structure. Consequently, soil properties do vary along the length of a pile and across the site.

- **Insufficient number of soil samples**

  This leads to error in the interpretation of the soil properties based on widely scattered locations in field, thus affect the averaged soil properties input to the analytical prediction model.

- **Systematic error of soil properties**

  Sometimes, despite the availability of a large amount of measured data, the estimation of the soil properties could still be subject to significant error.

The reason is simply that all the measurements made could have been consistently too high or too low due to common sample disturbance, calibration error of instrument, or other factors.

Load uncertainties could also be very large. An offshore platform subjects to environmental load induced by waves, wind and possibly earthquakes, which all have large inherent probability of variation. For example, the annual maximum wave height fluctuates considerably between years. This inherent variability is further magnified by the uncertain dynamic transfer function relating the wave characteristics to the induced loading at the pile head. The main loadings transmitted onto a pile head take the form of axial load, lateral load and possibly bending and torsion moments. However, the structure behavior at connection between jackets and piles is extremely difficult to predict. The forms and values of actual loading and boundary restraint on the pile have a large range of variation. Moreover, the patterns of cyclic degradation and high loading rate effects in the dynamic analysis are subject to insufficient understanding, thus involve large uncertainties in the pile capacity prediction.

Each pile capacity prediction method has some simplifying assumptions. This uncertainty is a system error which vary among different prediction methods. Experiments and field tests indicate that even if the soil parameters in the input to prediction model could be accurately determined and if the applied loads are carefully controlled, discrepancy would still prevail between the predicted and measure pile responses. Besides this, the numerical and discretization procedure in the current prediction model to solve the beam-column equation could also impose additional uncertainties. Furthermore, most present prediction models are correlated to the load test results to verify their validity. Thus the discrepancy between in site pile capacity during operation and those measured in load test program impose another uncertainties on the pile foundation analysis. The pile capacity measured at a load test does not necessarily have the same capacity of a similar pile during a storm. For instance, load tests are

generally performed within 100 days of pile installation, whereas the maximum load applied to a pile during a structure's lifetime may occur years after installation. For most normally consolidated clay where soil strength around a pile generally increases with time after pile installation, the capacity measured during load tests could significantly underestimate the actual pile capacity due to this reconsolidation effect. Generally the capacity measured during the load tests with relatively slower loading rate underestimate the actual pile capacity. Other factors can also be identified that would cause a discrepancy between the load test capacity and the actual capacity during operation, such as soil reconsolidation, pile compressibility, jacking error during load test, etc., thus increase the uncertainties in the prediction model. As an example, Table 2.1 summarizes the biases for axial pile capacities.

Table 2.1   Bias in axial pile capacity in normally consolidated clays

Component	Reference Condition	Actual Condition	Median Bias
Boring	Drill mud, heave compensation	Sea water, drill collars	1.2-1.3
Sampling	Push large diameter	Wire-line small diameter	1.5-2.0
Testing	Remolded, reconsolidated, direct simple shear	Unconfined compression	1.5-2.0
Strength characterization	Upper bound	Lower bound	1.5-2.0
Loading	Static	Storm wave earthquake	1.5-2.0 2.0-2.5
Analysis	Nonlinear finite element, t-z, q-z degrading	Limit equilibrium	1.2-1.3
age	10 years	10 days	1.5-1.8

This report summarizes the results and conclusions of the research effort on identifying the uncertainties in the prediction models by the means of comparing predicted capacities obtained from several methods.
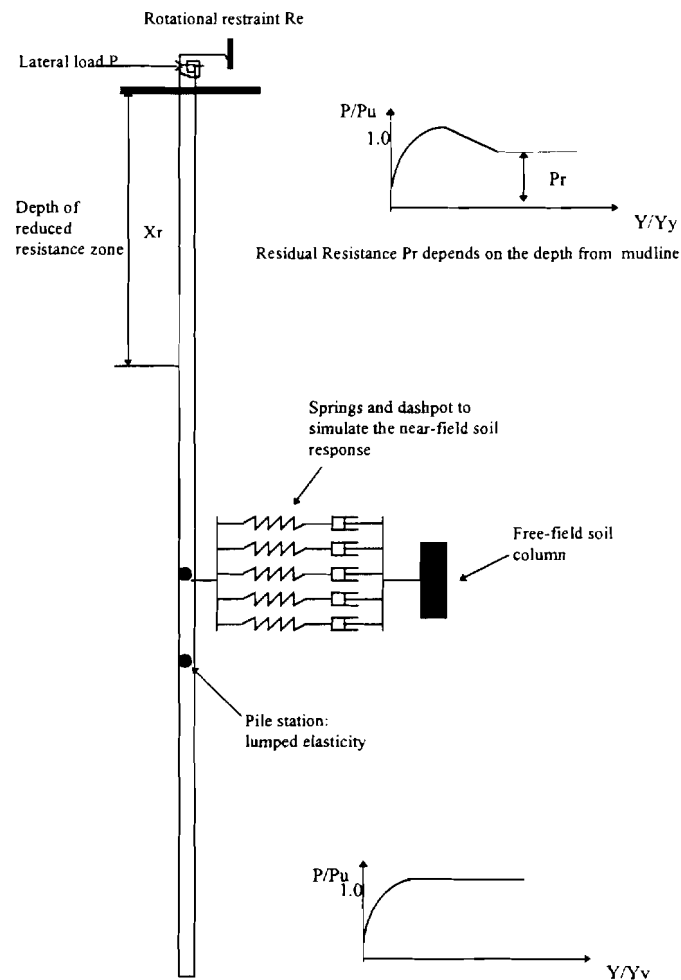
2.3   Analysis models in this study

The prevailing analytical models in use at present time are the discrete Winkler foundation model of beam-column based on non-linear soil support. Numerous researchers have studied the pile-soil capacity problems using this model(Matlock, 1978; Kagawa, 1986; PMB, 1988; Bea, 1992; Wang, 1996; Lok and Pestana 1997). This model is superior to the finite element model since its prediction fits the measured pile behaviors better. The Winkler foundation model is illustrated in Fig. 2.1. This study also takes the discrete element method as basic approach. There are two major prediction models in this study: the SPASM lateral response prediction model, and the more versatile analytical model developed by DRAIN3D structure analysis software package. The purpose of the these models is to investigate the ultimate behavior of the pile-soil system. ULSLEA is a simplified prediction model of the ultimate capacities of pile foundation.
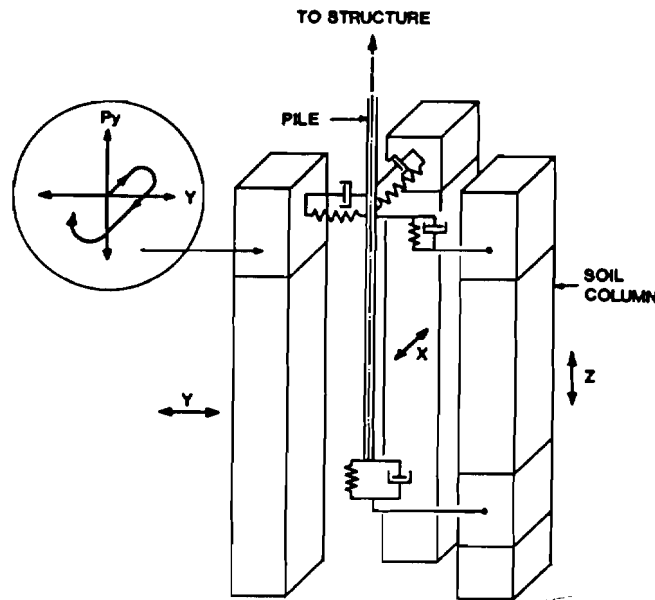
Fig 2.1   Winkler pile foundation model

2.3.1 SPASM model

There is a detailed description of the SPASM model used in this study in the earlier report of the first phase research (Jin and Bea, August, 1997). The basic mechanism of the model is shown in Fig. 2.2. This model has performed an excellent prediction of the lateral response of a single pile with different loading patterns and pile head rigidities, while the steel pile is still in the elastic range.

Fig. 2.2 Illustration of SPASM analysis model in this study

One thing shall be noted is that this model assumes an elastic pile in soils. The validity of the model is doubtable after the first yielding occurs in the pile. To keep a clear total picture of the pile response, this study assumes the steel pile exhibits an elastic-perfectly-plastic behavior. The second-order strain-hardening phenomenon is neglected. This means the stiffness of the pile will reduce to zero after yielding takes place. So there will be a significant loss in the stiffness of the steel beam-column based on non-linear soil supports. If the lateral load on pile element in the SPASM model keeps increasing after yielding, this analytical model will miss to capture the real deformation of the pile. However, theory and experiments have proved an ultimate collapse mechanism of such a beam-column. The pile will collapse after formation of two plastic hinges at certain locations along the pile length. For a beam with annular cross section and rotational fixed end, empirical and theoretical formulae have demonstrated the ultimate bending moment for such section is around 1.3 times the first yielding bending moment. Loading to this level will form the first plastic hinge in the beam. And it will usually take 1.4~1.5 times this loading to form the second plastic hinges. Based on this argument, an analysis by SPASM is performed to estimate the ultimate capacity of a laterally loaded single pile. It shall be emphasized that this analysis can only roughly capture the ultimate behavior of the pile with respect to the magnitude of loading at the pile head. Neither can it predict the real displacement of the pile head, nor can it indicate the final collapse patterns of the pile. The results from this study by SPASM are taken as a reference to the more powerful prediction model by DRAIN3D. They are also correlated to the ultimate capacity prediction obtained by ULSLEA. The detailed results are documented in Chapter 3.

2.3.2   DRAIN3D model

To evaluate the ultimate capacity of the pile foundation, especially for the case of laterally loaded pile, an analytical model which is capable of handling both non-linear

steel pile and non-linear-hysteretic soil support is needed. In this study, such a model is developed using the structure analysis software package DRAIN3D.

DRAIN3D(Dynamic Response Analysis of Inelastic 3-Dimensional Structures) computer program is a member of the family developed from DRAIN-2D at UC, Berkeley. The most recent version DRAIN3DX was developed in 1994. It is a powerful structure analysis tool for general use. The software package consists of a "base" program which manages the data and controls the analysis procedure, plus a set of subroutines for each element type which control the element details. Information is transferred between the base program and the elements through an interface that is the same for all the element types.

To perform an analysis of a structure, the structure is decomposed into an assemblage of 3-dimensional nonlinear elements connected at nodes. Nodes are identified by number, and need not be numbered sequentially. Each node has six degrees of freedom (translation and rotation). The elements are divided into groups. All elements in a group are of the same type. An element is identified by its group number and element number.

The structure mass is lumped at the nodes, and the mass matrix is diagonal. A viscous damping matrix that is proportional to the element stiffness and nodal masses can be specified. The form of this matrix is:

$$C = \Sigma \alpha M + \Sigma \beta K_{s} \qquad (2.1)$$

where M is the mass matrix, and K is stiffness matrix.

In effect, mass-dependent damping introduces translational and/or rotational dampers at each node, with damping coefficients α. Different values of α can be specified for each node of desired. Stiffness dependent damping introduces dampers in

parallel with the elements. Different values of β can be specified for each element group. The damping matrix, K_β, for any element, however, remains constant. In the current version of many elements, K_β, is set equal to the initial element stiffness, K_0. If desired, α and β values can be globally scaled between analyses.

The program uses an event-to-event strategy to solve the nonlinear problem, where each event corresponds to a significant change in stiffness. When an event occurs, the structure stiffness matrix is modified and an analysis is performed for the next step. It also permits a detailed energy balance calculation. This calculation accounts for the external work on the nodes, static elastic-plastic work on the elements, kinetic energy, and viscous damping work. If there is a significant energy unbalance, the analysis results are likely to be inaccurate. This scheme is simpler and more stable. But it requires more calculating time. To reduce the execution time, provision is made for event overshoot tolerances to be specified, so that the structure stiffness is not modified at each exact event but at a somewhat larger load.

Although the pile foundation response problem is principally a 2-dimensional problem, DRAIN3D is chosen over DRAIN2DX because the recent 3D version contains more versatile elements which are needed to simulate the unique stress-strain curve and cyclic degradation characteristics of the soil support. The elements contained in the recent DRAIN3D version element library are as follows:

- Element type 1: inelastic truss bar;
- Element type 4: simple connection element;
- Element type 5: friction bearing element;
- Element type 8: fiber hinge beam-column element;
- Element type 9: compression/tension link element;
- Element type 15: fiber beam-column element;
- Element type 17: elastic beam-column element;

The elements used in this analysis are element type 1, 4, 15. Type 1 element is a simple inelastic bar. It's nonlinear force-displacement curve can specified by defining the material properties of the bar. It can transmit axial load only. So it is an ideal element to
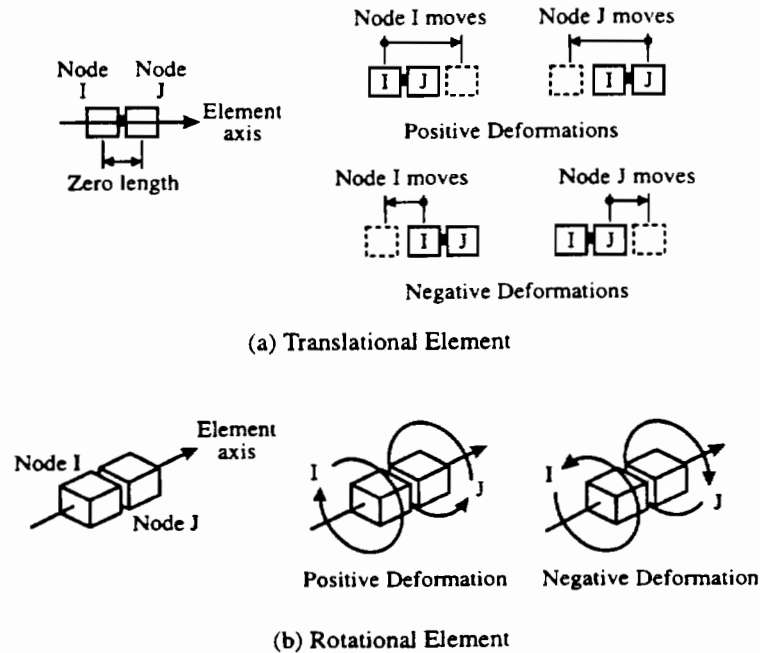

Fig 2.3 Illustration of the simple connection element used in Drain3D model

simulate the axially loaded steel pile. It is also used to represent the artificial rigid bar at each node by define a large stiffness coefficient. The purpose of such a rigid bar is documented in the next chapter.

Type 4 is a simple inelastic element for modeling structure connections with rotational and/or translational flexibility. It is used to form the elastic-perfectly-plastic spring group parallel or vertical to the pile axis direction to simulate the total t-z(or q-z) curves and p-y curves respectively. It is also used to specify the rotational restraint at pile head. The mechanism of this element is quite simple thus doesn't cost much calculation time. However, this element has no capability to simulate the displacement softening of

the soil. Thus it is not suitable to use for the case of cyclic lateral loading and the axial loading analysis. A simple illustration of the mechanism of this element is given in Fig. 2.3

Type 15 is the most useful element, but also the most complicated one. The element of this type is further divided into a set of sub-elements. There are a lot of choices to define various sub-elements to simulate different element behavior. A typical sub-element configuration is illustrated in Fig 2.4. The deformable part of the element is divided into segments. The behavior is monitored at the center cross section("slice") in each segment. The cross section properties are assumed to be constant within each segment, but can vary from segment to segment. Each cross section is either elastic or is divided into a number of fibers. The fibers can have non-linear stress-strain relationships for various types of material. The typical stress-strain curve can be used in the element is shown in Fig. 2.5. Note that it has the ability to handle the displacement softening of the material. It also has degradation feature in strength and stiffness of the connection hinge
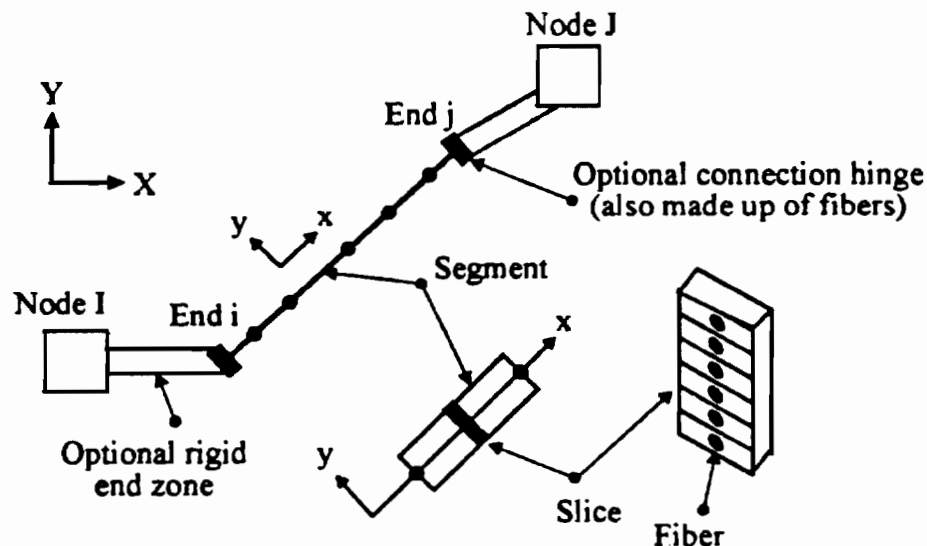
Fig. 2.4 Element type 15 in Drain3D model: nonlinear beam with distributed plasticity

in the element. By specifying the inelastic unloading pattern, the hysteretic damping is involved automatically. By determining the value of the viscous damping coefficient β, a dashpot parallel to the element is added implicitly to the element. This feature can represent the radiation damping of the soil. This element is used widely in the DRAIN3D pile foundation model to simulate the complicated supporting behavior derived from the near-field soils.
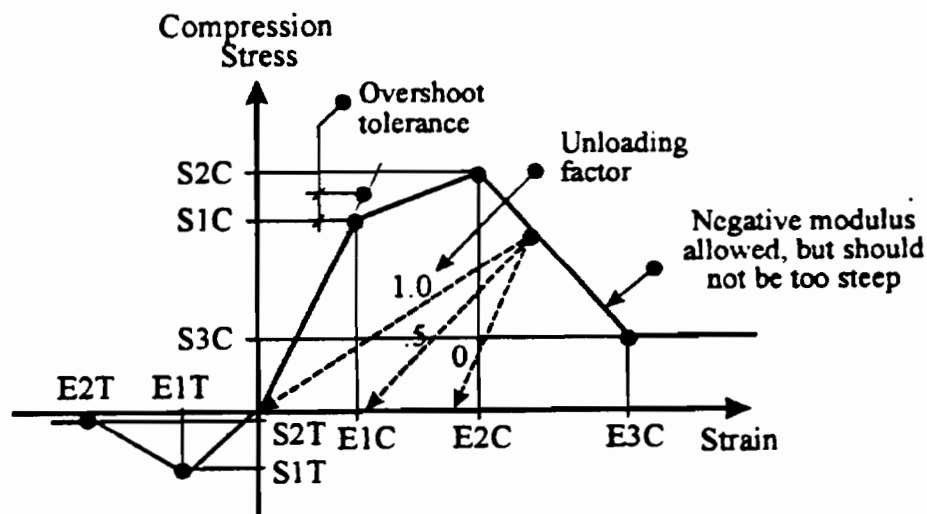
Figure 2.5   Typical "concrete" material stress-strain properties for the soil beams in Drain3D pile foundation model

Properly use of these elements can form a structure frame that can numerically simulate the combined pile-soil system response to lateral and axial loading. The layout of such a structure frame is different for these loading cases. The detailed description of these frames is documented in chapter 3 and 4.

2.3.3   ULSLEA MODEL

The ULSLEA program is a simplified screening method for use in the platform assessments and requalifications. It has subroutines calculating the static lateral and axial capacities of the pile foundation. The current version of ULSLEA (V. 3.0) assumes that the foundation soil of either exclusively cohesive L(with variable soil shear strength) or exclusively cohesionless. The Phase IV ULSLEA will modify the current pile capacity strength formulation to allow for the ultimate lateral and axial strengths of a pile imbedded in separate layers of cohesive and cohesionless material to be estimated.

Lateral Pile Capacity

In ULSLEA phase IV, a pile is assumed to reach its lateral capacity when plastic hinges form at the mudline and at some depth where the moment on the pile reaches the fully plastic bending moment. By considering the soil at each incremental length along the pile to absorb load up to the soil's maximum bearing capacity, the point of zero shear in the pile can be estimated; this is also the point of fully plastic bending moment in the pile. Therefore, the depth at which the maximum moment occurs determines the length of the pile with which the collapse mechanism is formed. This mechanism is shown in Fig. 2.6.

The pile ultimate lateral load and the point of zero shear force L_d may be related by integrating the incremental soil resistance S_u over the presumed L_d :

$$P_. = \int_0^{L_d} S_.(z)dz \qquad (2.2)$$

Using virtual work, another equation relating the point of zero shear force and the pile ultimate lateral load can be developed:

$$P_{u,l} = \frac{2M_p}{L_d} + \frac{1}{L_d} \int_0^{L_d} S_u(z)z\,dz \qquad (2.3)$$

Equating the two relations by dropping L_d allows $P_{u,l}$ to be related to the plastic moment capacity of the pile M_p and the cumulative soil resistance. The above approach has not been coded into ULSLEA. But the calculation can be done by a spreadsheet. The calculation results are documented in Chapter 3 as a comparison with ULSLEA V.3.0.
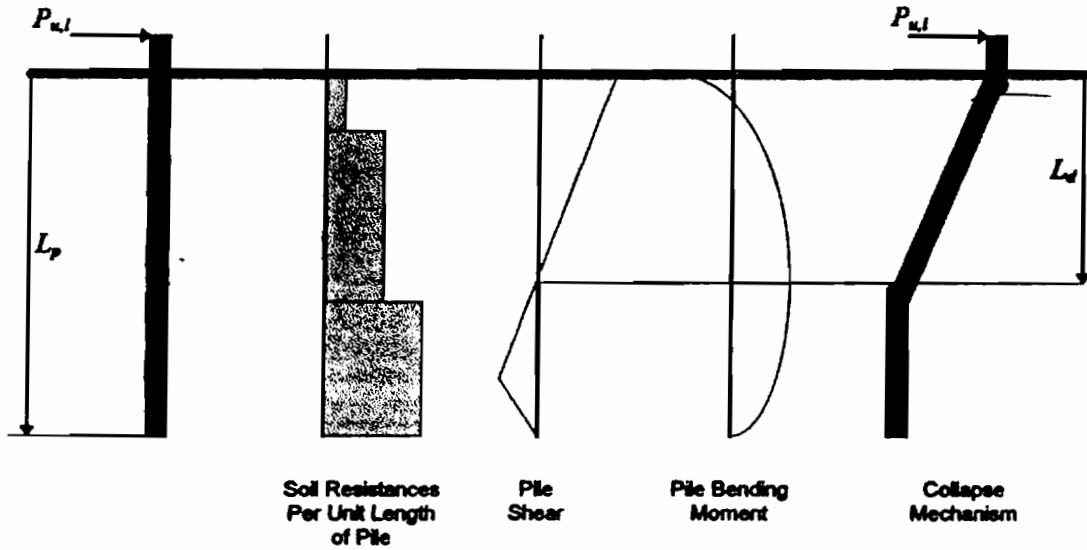
Figure 2.6   Illustration of collapse mechanism for laterally loaded pile

The formulae used in ULSLEA 3.0 have been documented by Mortazavi (1996). Following is a brief summarization for the case of linear increasing strength with depth, which is an estimation of the soil characteristics in the Bay of Campeche.

For this case, the ultimate lateral capacity of the pile, $P_{u,l}$, can be estimated from the following equation:

$$P_{u,l}(C+\xi) - 2M_p - (A+\eta\xi)\frac{C'}{2} - \left(\frac{\eta}{2}\right)\frac{C'}{3} = 0 \qquad (2.4)$$

20

where

$$C = \frac{1}{\eta}\left[(-A + \eta\xi) + \sqrt{(A + \eta\xi)^2 + 2\eta P_u}\right]$$

$$\eta = \frac{B - A}{L_p}$$

$$\xi = 15D + X$$

$$A = 9S_{u1}D \text{ and } B = 9S_{u2}D$$

S_{u1} and S_{u2} denote the undrained shear strength at mudline and at the pile tip respectively.

Vertical Pile Capacity

In ULSLEA v. 3.0 and Phase 4, a pile is assumed to reach its vertical capacity when all vertical resisting mechanisms (shaft friction and end bearing) have yielded. The axial resistance of a pile is based on the combined effects of a shear yield force acting on the lateral surface of the pile and a normal yield force acting over the entire based end of the pile (Figure 2.7). Thus the ultimate axial capacity Q_u, can be expressed as:

$$Q_u = Q_p + Q_s = qA_p + f_{av}A_{sh} \tag{2.5}$$

Q_p denotes the ultimate end bearing and Q_s is the ultimate shaft capacity, q is the normal end yield force per unit of pile-end area acting on the area of pile tip A_p, and f_{av} denotes the ultimate average shear yield force per unit of lateral surface area of the pile acting on embedded area of pile shaft A_{sh}. It is assumed that the pile is rigid and that shaft friction and end bearing forces are activated simultaneously. It is further assumed that the spacing of the piles is sufficiently large so that there is no interaction between the piles.

After considering the weight of the pile and the soil plug (for open-end piles), the ultimate compressive loading capacity of the pile, Q_c, can be calculated as:

$$Q_c = \frac{q_u \pi D_o^2}{4} + \left(f_v \pi D_{-o} - W_p\right)L_p \tag{2.6}$$

$$W_p = \gamma_{st} A_{st} + \gamma_s A_s = \frac{1}{4}\left[\gamma_{st} \pi(D_o^2 - D_i^2) + \lambda_s \pi D_i^2\right]$$

where

A_{st} = cross-sectional area of the steel pile

A_s = cross-sectional area of the soil plug

D_0 = outside diameter of the pile
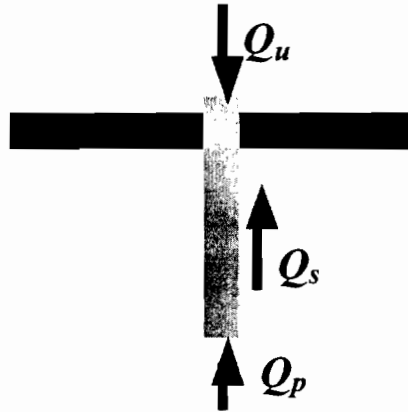
D_i = inside diameter of the pile

f_v = yield stress

γ_{st} = submerged specific weight of steel

γ_s = submerged specific weight of soil

L_p = pile embedded length

W_p = weight of pile and soil plug per unit length

Figure 2.7 The ultimate axial pile response

22

The end bearing capacity can be fully activated only when the shaft frictional capacity of the internal soil plug exceeds the full end bearing (Focht and Kraft, 1986). This condition can be formulated as:

$$\frac{q\pi D^2}{4} \triangleleft \left(f_o D_o + W_i\right)L_p$$

For cohesive soils with an undrained shear strength, S_u, the ultimate bearing capacity is taken as the bearing of a pile in clay

$$q = 9S_u$$

The ultimate shaft friction is taken as

$$f_m = kS_{uav}$$

where k is the side resistance factor and a function of the average undrained shear strength S_{uav} as given in Table 2.x.

Table 2.1   Side resistance factor formulated in ULSLEA 3.0

Undrained shear strength $S_{u,av}$(ksf)	Side Resistance Factor K
< 0.5	1
0.5 - 1.5	1-0.5
>1.5	0.5

The above approach is similar to that suggested in the API RP-2A guideline except the side resistance factor. The API guideline has a effective overburden pressure approach. For Pile piles in cohesive soils just as the soils in the Bay of Campeche, the shaft friction f, in lb/ft^2(kPa) at any point along the pile may be calculated by the equation,

f = αc

where:

α = a dimensionless factor

c = undrained shear strength of the soil at the point in question

The factor, α, can be computed by the equations

$$\alpha = 0.5 \, \psi^{-0.5} \quad \psi \leq 1.0$$

$$\alpha = 0.5 \, \psi^{-0.25} \quad \psi > 1.0$$

with the constraint that, $\alpha \leq 1.0$,

where:

$\psi = c/P_0'$ for the point in question

P_0' = effective overburden pressure at the point in question lb/ft^2 (kPa)

As a comparison, the ultimate axial capacity calculation follows the API guideline is also performed and documented in Chapter 4.

Chapter 3

Lateral Pile Response

3.1   Set up of the analysis models

Three analysis models are used in the study of the lateral response and capacity characteristics: SPASM, DRAIN3D, and ULSLEA. The set-ups of these models are almost the same except some different special input to them. Following is a general description of the inputs and configurations of the models of the pile-soil systems.

3.1.1   Pile parameters, load patterns and soil profiles

The pile in this study has the same material parameters and geometry characteristics as that documented in the phase 1 report (Jin and Bea, August, 1997). The pile has a penetration of 200 feet. The diameter is 4 feet. The thickness of the pile wall is 1.5 inches. The discretization procedure of the pile is also the same. The pile is divided into 50 uniform segments. The pile head rigidities in study are the same as those of phase 1 works: rotationally fixed, free, grouted (3E+10lb.in/rad), and shimmed (5.25E+9lb.in/rad).

The loading patterns are kept the same for the sake of comparison to the phase 1 results. Three cases studied are static, quick and cyclic lateral load at pile head with different head rigidity. The pile is loaded to the point of the first yielding at the same rates as those in the previous work. This study keeps increasing load at pile head after the first yielding occurs in the pile, until the final collapse of the pile.

25

The input soil profile under study is taken from the phase 1 study, which is based on the soil investigation information provided by PEMEX and IMP. The relationship of undrained shear strength vs. depth below mudline is plotted in Fig. 3.1.

3.1.2 Configuration of the pile-soil models

SPASM Model

There is no change to the set-up of the SPASM model, the p-y curve for each stratum of the soil is simulated by the combined action of the elastic-perfectly-plastic springs at each pile node. Based on the argument stated in chapter 2, the pile in SPASM model is loaded to the state that the bending moment at certain pile nodes reaches 1.5 times the ultimate bending moment across the pile section. The load values are taken as estimation of the ultimate capacity the pile-soil system can develop. The analysis results are compared with DRAIN3D and ULSLEA in the following sections.

DRAIN3D Model

The DRAIN3D pile-soil model is a completely new one. As DRAIN3D is a general analysis program mainly dealing with the non-linear structure problems of buildings, it's set up is not as convenient as the specific soil mechanics programs such as SPASM. The pile-soil system is translated into an equivalent "solid" structure frame just the same as the steel-concrete structures in building. The equivalent structure in this study is a truss frame, which is an assemble of beams, columns, bars and nonlinear connections. The configuration of such a truss frame is shown in Fig. 3.3.

In the truss frame shown in Fig. 3.3, the only "real" component is the vertical column that represents the steel pile. This pile consists of 50 type 15 elements. As the

failure of the pile-soil system is not owed to the failure of soil supports, but the formation of plastic hinge in the pile, the cross section is divided into 8 non-linear fibers, which can simulate the plastic behavior of the pile segment after yielding take places. The features of these fibers are carefully determined so that the geometry properties of the cross section, such as cross area, section modulus, principal axis, do not change. The readers can refer to Fig. 2.5 and Fig 3.2 for the details of such pile elements.

The supporting beams in the truss frame are added to each pile node to simulate the non-linear-hysteretic soil resistance. They are artificially "faked" elements. Their responses to loading are carefully evaluated to guarantee that the force-displacement relationship at each pile node is consistent with the specified p-y curve in that soil layer. The material of these beams are of typical "concrete" type in DRAIN3D element library, which are at least tri-linear in compression and can simulate the displacement softening phenomenon. That means the modulus of such an element may become negative if strain is larger than certain value. This softening may induce a problem of numerical stability in calculation that shall be solved by certain means. The stress-strain curve of this kind of "concrete" material was plotted in Fig. 2.4. Note that the shape of the curve is just the same as the shape of a t-z curve with softening after the peak stress, or the cyclic p-y curve. As the t-z curves and p-y curves reflect the force-displacement relationship, care shall be taken to transfer the stress-strain curve of the element material into force-displacement curve. Since the supporting beams are under compression, the following formula is used to relate the stress-strain curve to force-displacement curve:

$$\Delta = \frac{P}{AE} L \qquad (3.1)$$

Where, Δ is the displacement, L is the element length, P is the axial force on the element, E is the stiffness, A is the cross section area. E can be easily determined according to the coordinates in the p-y curves. L shall be large enough so that the strain can be calculated directly, assuming the total deformation of the element is small. The

possible maximum deformation in the near-field soil is 15 times y_c, i.e., 1.5 feet. So the beams simulating the p-y springs are set to be 15 feet long so that the total strain is at most 10%. In this range of strain, equation 3.1 is regarded valid.

In Fig. 2.4, the stress-strain curve are not two-way symmetrical, meaning that the typical "concrete" material in DRAIN3D does not exhibit the same response to compression as to tension. So the supporting beams in the truss frame are specified to have no resistance to tension. Meanwhile, as shown in Fig 3.2, two such beams, one on each side, are attached to each pile node. The combined response of the two beams can simulate the two-way symmetric soil p-y springs.

During the build-up of the DRAIN3D model, one unexpected problem showed up. The calculation algorithm of DRAIN3D is so detailed and delicate that it can reflect the complicated distribution of forces and moments among the elements connected at each node. This is desirable in a real structure analysis, but not desirable in the simulation of the soil resistance. The earlier DRAIN3D models in this study have no rigid bar(refer to Fig 3.2) at each node. Analyses by these models always could not be loaded to the ultimate state. They stopped before the formation of the second plastic hinge in the pile. A careful examination of the input and output turned out that the beams simulating the soil resistance were unstable at those stop points. The beams buckled under compression just as what may happen in a real building structure. Obviously, this is not true for soil resistance. The near-field soils never buckle. Their response to external load follows the special p-y curves. The simulation of the soil resistance by plastic beams fails at the stop points. Several attempts were tried to solve the problem: such as change the beams' length, increasing the cross section area. The purpose is to stabilize the beams by increasing the Euler stress. But all these efforts yielded no positive results. Finally, the buckling was traced to the distributed bending moment from the node to the beams. When the pile bends under lateral loading. Bending moments are created at each pile node. In the calculation algorithm in DRAIN3D, a small portion of this moment is

28

distributed to the beams. This means that the beams are under combined action of axial compression and bend moment. According to the structural mechanics, we know the disturbance of small external bending moment can greatly reduce the Euler stress thus lead to much earlier buckling of the compression beam. This conclusion is supported by the fact that the instability always takes place in the first segment of the beams, which is connected to the pile node. The deformation in this segment is much larger than the rest ones. To get rid of the unnecessary small bending moment, short rigid bars are added to connect the pile node to the soil supporting beams. The connection nodes between these rigid bars and beams are specified to have only one degree of freedom. The connections are rotationally fixed so that only the axial force can be transferred to the supporting beams. The function of these rigid bars and the restrained connection nodes can filter the undesirable disturbance of the small bending moments. The illustration in Fig 3.2 gives details of the configuration of the elements, their sub-elements, connections and rigid bars at each node.

In Fig 3.3, the material for the supporting beams at each pile node are set to have their special stress-strain relationship to simulate the characteristics of p-y response of the layered soils. The radiation damping of the soils is implicitly simulated by the viscous damping in each element. The rotational restraint at pile head can be obtained by adding a type 4 rotation simple connection at pile head. The external loading at pile head can be either displacement-controlled or load-controlled. Load control pattern is used to calculate the elastic response of the pile. After the pile is loaded to the point of the first yielding. The load pattern is changed to displacement control to capture the ultimate response of the pile. This is because that there are a lot of elements, both pile segments and soil supporting beams, yield during this loading process. When the second plastic hinge is being formed in the pile, a small increase in the loading may cause a very large displacement. This is another   reason why the displacement control pattern is applied in the ultimate state analysis.

The DRAIN3D model can predict the response of the pile-soil system. Based on the set-up of the model described above, three kinds of loading case are studied separately: static, fast and cyclic.

3.2   Lateral response of a pile to the static loading

The present approach used in the design of pile foundation has a pseudo-static style. The static response of the pile-soil system is the basis for more realistic in-field response. Analyzing and understanding the static response of such piles is a principal problem in analyzing and understanding their dynamic response. This is because that the static response is a critical element in realistic loadings that can be characterized as being static on those that are dynamic. Also, if one does not properly understand the response of a system to its static loadings, it is unlikely that one can properly understand the response of the system to its dynamic loading. The two philosophical and analytical frameworks are complementary and necessary to each other.

3.2.1   First yielding capacity obtained by SPASM and Drain3D

There are usually three failure modes in lateral pile design. The first is excessive displacement at the pile head, which may affect the production equipments thus cause the loss of serviceability of the platform system. The second is the initial yielding of steel pile, which causes permanent deformation in file. The third is the final collapse of the steel pile resulting from formation of plastic hinges.

The first yielding capacities of the pile calculated by SPASM have been summarized in the phase 1 report. The results of static loading analysis are shown in Table 3.1.

The first yielding capacities were also calculated by Drain3D model. The results are also showed in Table 3.2. It can be seen that there is a great agreement between the results from two models.

3.2.2 Ultimate capacity

The ultimate capacity is the focus of this study. The static lateral ultimate capacities for the four different cases of pile head rigidities are predicted by three computer programs: SPASM, Drain3D and ULSLEA. The Drain3D model is the most detailed model and is regarded as the "exact" prediction method. ULSLEA is the simplified estimation of the static ultimate capacity. Amazingly, the prediction by this very simple model has very good agreement with the complicated Drain3D model. The results by SPASM and Drain3D are shown in Table 3.1 and Table 3.2. The detailed force-pile head displacement relationship is shown in Fig. 3.4.

3.3 Lateral response of a pile to the dynamic loading

Two dynamic load patterns are studied. As explained in the phase 1 report. The SPASM model has a time-history approach for both fast loading. The model directly incorporated the load rate effect in the modified p-y curves based on the static backbone p-y curves. The same approach is taken in the Drain3D model for the case of fast loading. For the cyclic loading, SPASM still has a time-history approach. The cyclic loading effects are reflected by the cycle-by-cycle degradation mechanism suggested by Matlock. The Drain3D model uses a different approach. The cyclic p-y curves modified from the static backbone curves are used in the model. It is intended to capture the residue ultimate capacity when the final equilibrium state of soil characteristics is reached after a large number of load cycles.

31

3.3.1 Fast loading

The results from SPASM and Drain3D are summarized in Table 3.1 and Table 3.2. The Fast loading analysis by SPASM gives somehow overestimated ultimate capacities compared with those by Drain3D. This is due to the estimation method by SPASM is based on the static response of the pile. It is questionable whether this method works well for dynamic problem. The calculation results have proved this doubt. Using an overestimated pile stiffness in the plastic range results in an overestimated ultimate capacity for the dynamic loading. The pile head displacement is much underestimated thus the pile can survive much longer than it should be.

The Drain3D model gives more reasonable prediction. The time-history record of the fast loading to the final pile collapse is shown in Fig 3. 5. Comparing this figure with that similar one obtained by SPASM in phase 1 report, the agreement between them before initial yielding is significant. After the first yielding, the SPASM model is no longer valid in predicting the ultimate response. The ultimate response calculated by Drain3D is more realistic. In Fig 3.5, a normalized loading factor P/P_u is plotted vs. pile head displacement for all cases of pile head rigidities. When P/P_u reach the value of 0.95, the second plastic hinge is in the procedure of formation. Keep increasing loading on the pile head, the pile head displacement will increase dramatically. This is the obvious indication that the collapse of the pile take places. It can be seen that the fixed and restrained pile head cases have almost the same ultimate capacities. The case of free pile head has a much lower capacity because the failure mechanism is quite different from other cases. For free pile head, the pile-soil system will collapse shortly after the formation of the first plastic hinge, when all the supporting beams in the top soil layers fail. The ultimate pile head displacements are in the range of 1.1-1.3 feet. The variation is very small, not like what is expected before the calculation. From Fig. 3.5, another thing shall be noted. For large pile head rigidity, such as the cases of fixed and grouted pile heads, the initial yielding occurs earlier in the loading history than the small rigidity

cases such as shimmed and free pile head. This means the later cases have smaller residue strength after initial yielding. For the practice of pile design, these conclusions are meaningful. If you design a pile with large pile rigidity(grouted pile head), the boundary restraints of the pile is so stiff that the first yielding is easy to take place in the pile. The pile tends to suffer permanent deformations at relatively lower loading. But it has a large portion of reserve strength. It has enough robustness to resist additional loading. On the contrary, the pile with small pile head rigidity is more flexible. It is not easy to yield thus can avoid permanent deformation at high loading. However, it has small reserve strength. The ultimate strength is just a little higher than the initial yielding strength. For this kind of pile, it is very dangerous if yielding take place in the pile. The pile has no robustness.

3.3.2 Cyclic loading

As to the cyclic loading, the ultimate capacities obtained by SPASM and Drain3D are listed in Fig. 3.6. Comparing the time-history record of the SPASM and Drain3D in the elastic range, one can find that they are comparable. Although the two models have different approaches, there is a good match between them in the prediction of initial yielding capacities and pile head displacements. The application of the cyclic p-y curve can reflect the final fully degraded soil characteristics. In the plastic range, only the prediction of Drain3D is considered as valid. The SPASM results are overestimated.

In Fig 3.6, it can be seen again that the cyclic ultimate capacities of the pile are almost the same except the free pile head. Compared with the fast loading results, the ultimate capacities are much lower. This is because the support from the soils is much lower than the former case. The pile take a much larger portion of the loading thus develop plastic hinges much earlier at lower external loading. But the ultimate pile head displacements are still in the range of 1.1-1.3 feet. This is a implication that there is a maximum lateral pile head displacement for the pile-soil system under study. This may

33

be an important conclusion. More study of different pile configuration and soil profiles are needed to prove the generality of this conclusion

3.4   Correlation with ULSLEA

As to the static ultimate capacity, there are several kinds of calculation methods in this study. Drain3D is the complicated one, trying to simulate all the details of the ultimate lateral pile response. ULSLEA is a simplified approach. It considers the ultimate state of the pile-soil system. By introducing the virtual work principle, the complicated fully plastic problem is simplified to only two equilibrium equations, one for force, the other for bending moments. ULSLEA gives quite good estimation of the static ultimate capacity of the pile and the location of the second plastic hinges. The comparisons of the results by different methods are listed in Table 3.1, Table 3.2 and Table 3.3. By correlating the ULSLEA results with those from the complex models, one amazing fact turns out that the predicted capacity values are quite close. This is an implication that the simplified models such as ULSLEA can assess the pile capacity as well as the advanced, complicated model such as Drain3D. A more surprising phenomenon can be observed by correlating the ULSLEA and Drain3d results. The ultimate pile capacity and pile head displacement are not sensitive to the pile head rigidity if the pile head restrain is large enough. The difference between the fixed, grouted and shimmed pile head does not cause much difference in the final ultimate state of the pile soil system. Of course, the free pile head behavior predicted by Drain3D is quite different from the restrained pile head. Is seems the ultimate capacity will become sensitive to the pile head rigidity if the rotational restrain from the jacket drops to a very low value. However, the piles in field never have free pile heads. They are at least shimmed. The rotational restrain is usually in the unsensitive range. This implies that the ULSLEA can give a very good estimation of the pile lateral ultimate capacity no matter what kind of pile head rigidity presents. In the offshore engineering practice, the difficulty in estimating the stiffness at the connection between the pile head and the superstructure has been cognized for a long time.

34

Considering the fact that there is a large amount of uncertainty in determining the pile head rigidity in field, the above conclusion has great practical value. Again, the ULSLEA model demonstrates its advantage of simplicity and correctness.

3.5 Summary

Tang(1990) performed a systematic reliability analysis of the lateral response of the offshore pile foundation. He defined three performance criteria for laterally loaded pile. Namely, they are the displacement mode(excessive displacement at pile head), the damage (first yielding) mode, and the collapse (ultimate yielding)mode. His analysis assumed an elastic pile, thus they are valid only up to first yielding. This study extends the analysis scope to the plastic range. The analysis results have demonstrated that the three failure modes are inherently related.

As to the displacement criteria, a surprising conclusion drawn from the analysis results is that there exists a maximum pile head displacement for the pile under study. Given the pile configuration and soil characteristics, the pile-soil system in this study has a maximum displacement ranging from 1.1 feet to 1.3 feet for different pile head rigidities and loading patterns. The range is very narrow considering that there are large variation in pile head rigidities and loading patterns. So, it can be concluded that the pile will be doomed to fail if this maximum displacement is exceeded. This concedes with the empirical displacement criteria that the maximum pile head displacement is 1 foot to maintain the serviceability of the platform systems. More case studies of different pile configuration and soil profiles will be conducted to see whether the above conclusion is generally applicable.

The displacement criteria are related to the pile head rigidity. The pile rigidity greatly influences the damage criteria. When the initial yielding occurs, the lateral loading and the pile head displacement at that point are quite different for different pile

35

head rigidities. For the large pile head rigidity, the first yielding occurs earlier during the loading process. The displacement at the point of first yielding is relatively small. But the pile has large porting of reserve strength. The pile with small head rigidity is the contrary case. The displacement at the first yielding is relatively large. The first yielding occurs later. But this kind of pile has small reserve strength. In one word, the more rigid piles are prune to suffer permanent damage, but not easy to collapse; while the more flexible piles can stand large loading without suffering permanent damage, but tend to collapse quickly after the occurrence of the first yielding.

The collapse criteria is amazing the same for the restrained pile head, no matter how large is this restrain. The ultimate lateral capacities of the pile are almost the same. The ultimate displacements are almost the same too. The free pile head case is an exception. But this case is just a sensitivity study, which can not and shall not be achieved in field.

The bending moment distribution has typical patterns for the cases of first yielding and ultimate collapse. Such typical patterns obtained by Drain3D are plotted in Fig. 3.7 and Fig 3.8. Note that the bending moment distributions at collapse are the same for restrained pile head except the positions of the second plastic hinges. For different pile head restrain and loading pattern, the positions of the second plastic hinges vary from 11th pile node to 13th pile node, i.e., 44 to 52 feet below the mudline. This value is comparable with the prediction of ULSLEA, which is 39 feet for the fixed pile head.

As to the loading rate effects, the increase in the strength and stiffness of the soils results in an increase in the first yielding and ultimate collapse capacities compared with the static capacities. The soils provide larger supporting to the pile. More lateral loading will be transferred to soils. Again, no matter how large is the pile head restrain for this case, the ultimate capacities keeps the same. This implies that the increase in the soil resistance is not large enough. After the formation of the first plastic hinge in the pile,

the pile stiffness drops drastically. The boundary condition of the head restrain becomes less important. The pile can not take as much loading as before. But the increase in soil strength by loading rate effect is not strong to take the additional loading. This is the reason why the ultimate collapse states are similar for different cases of the pile head rigidity. The collapse failure mode of the laterally loaded pile involves mainly yielding of the pile itself instead of the soil, the loading rate effect is not as important as for the axial pile capacity.

As to cyclic degradation, the soils can only provide the residue resistance to the pile after they are fully degraded. The typical value for residue resistance of the soils in the Bay of Campeche is 70-80%. The cyclic first yielding and ultimate collapse capacity suffer a decrease. Both approaches of loading time-history in SPASM and the equivalent cyclic p-y curves in Drain3D produce results with good agreement. They capture the lower bound of the residual soil resistance that can be developed during the cyclic degradation. The lower bound capacities of pile-soil system under cyclic loading are roughly 65-80% of the static capacities.

Tables and Graphs

Table 3.1 Lateral capacities calculated by SPASM

Lateral capacities of a single pile (CALCULATED BY SPASM)						
	First Yielding Capacity (kips)			Ultimate Capacity(kips)		
Head Rigidity	Quasi-static	Quick	Cyclic	Quasi-static	Quick	Cyclic
Fixed Head	479	550	453	813	968	778
Free head	383	460	359	627	871	599
Grouted	525	618	496	867	1073	831
Non-grouted	630	740	599	1046	1400	1002

Table 3.2 Lateral capacities calculated by Drain3D

Lateral capacities of a single pile (CALCULATED BY DRAIN3D)						
	First Yielding Capacity (kips)			Ultimate Capacity(kips)		
Head Rigidity	Quasi-static	Quick	Cyclic	Quasi-static	Quick	Cyclic
Fixed Head	513	609	413	765	895	645
Free head	415	472	351	489	537	400
Grouted	480	645	453	765	895	641
Non-grouted	643	725	554	765	895	645

Table 3.3 Ultimate capacities calculated by ULSLEA

Static ultimate capacity of a single pile (CALCULATED BY ULSLEA)	
Fixed Head	**ultimate Capacity(kips)**
ULSLEA 3.0 (linearly increasing S_u)	793
ULSLEA phase IV(layered soils)	910
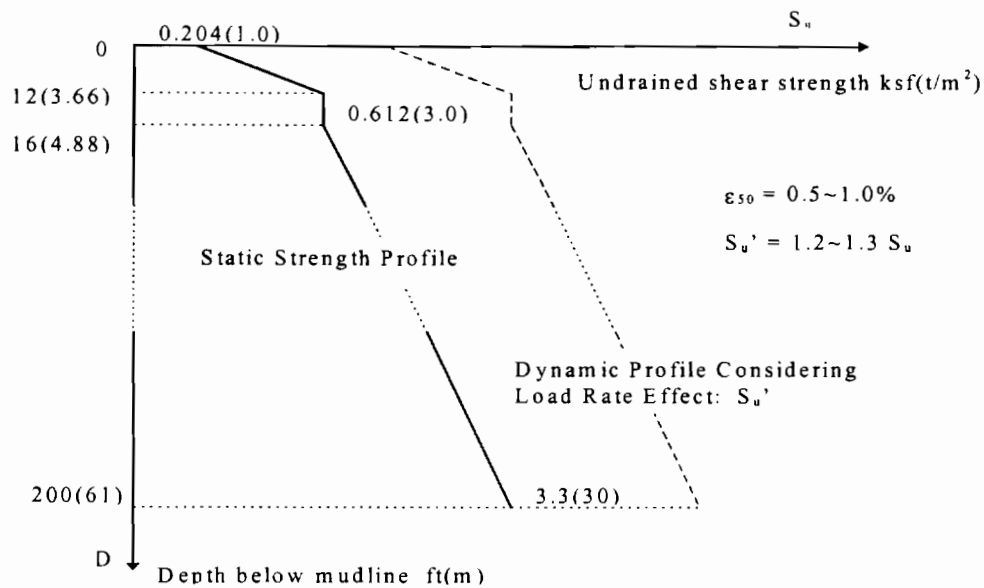
Figure 3.1 Typical soil profiles in the Bay of Campeche
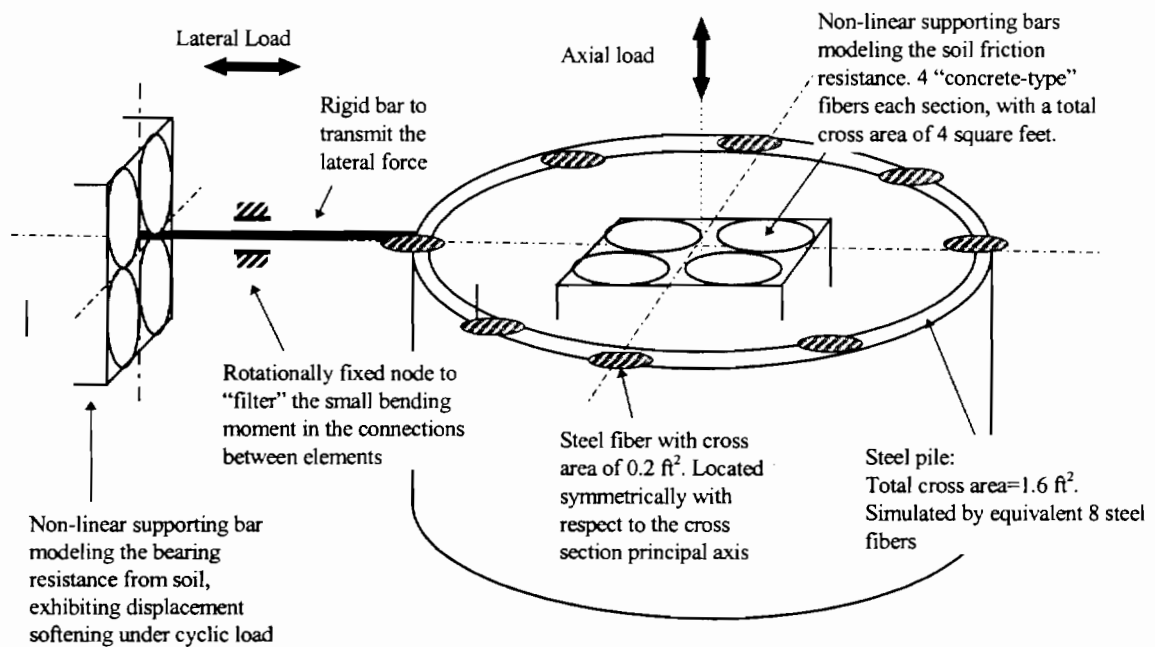
**Figure 3.2 Details of the configuration of elements and sub-elements
at pile node**
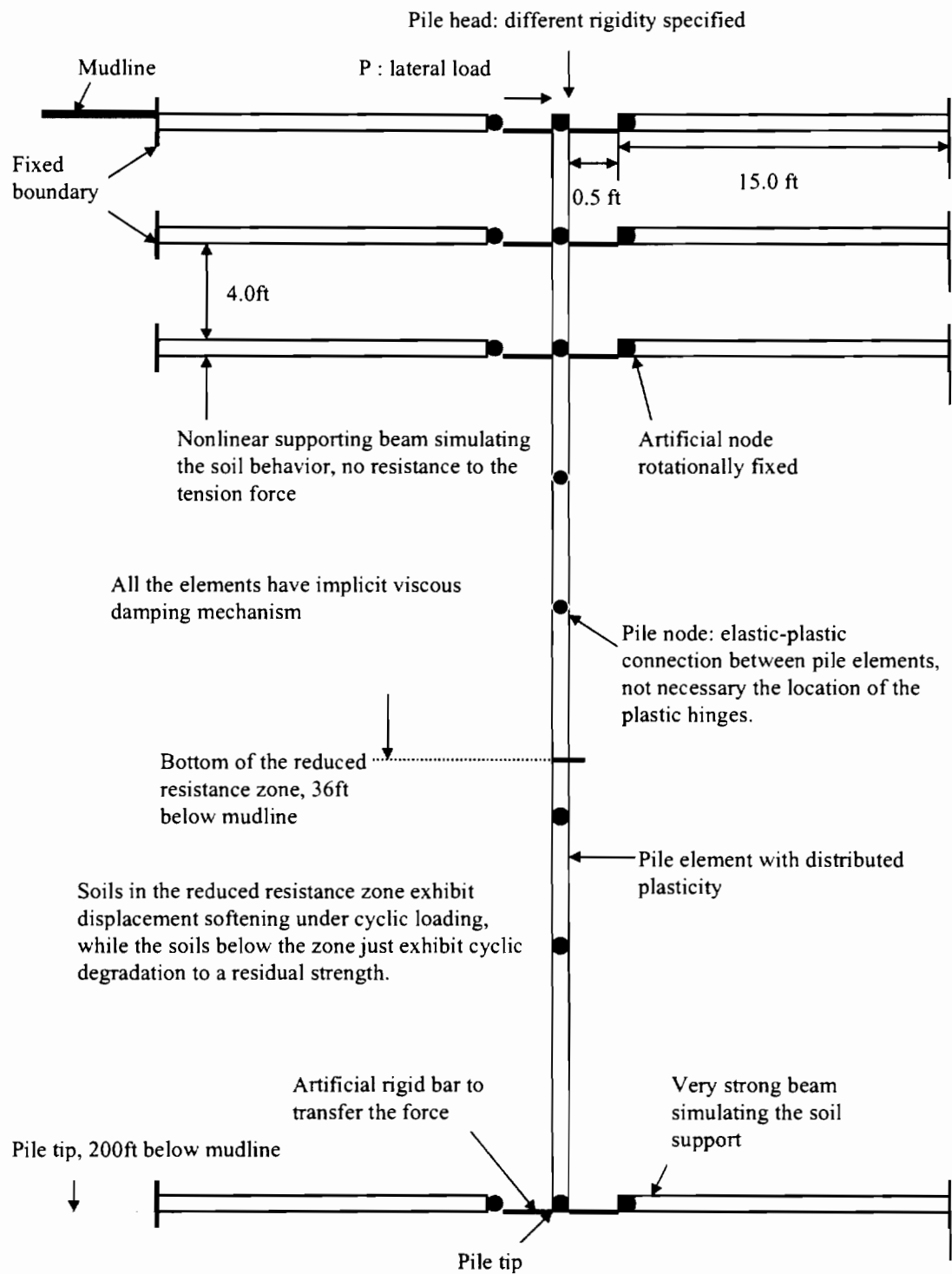
Figure 3.3   Equivalent truss frame in Drain3D simulating the p-y response of the
pile-soil systems

Ultimate Static P-Y Response:
Normalized loading factor vs pile head displacement
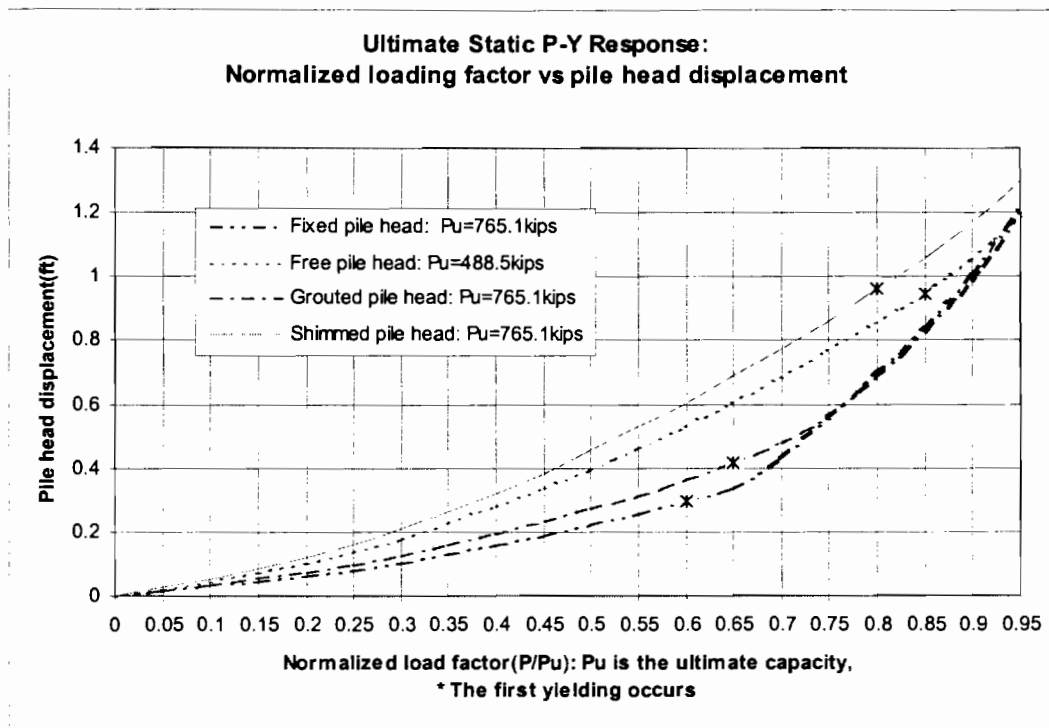
Figure 3.4 Displacement-loading relationship for static loading

Ultimate P-Y Response to Fast Loading:
Normalized loading factor vs pile head displacement
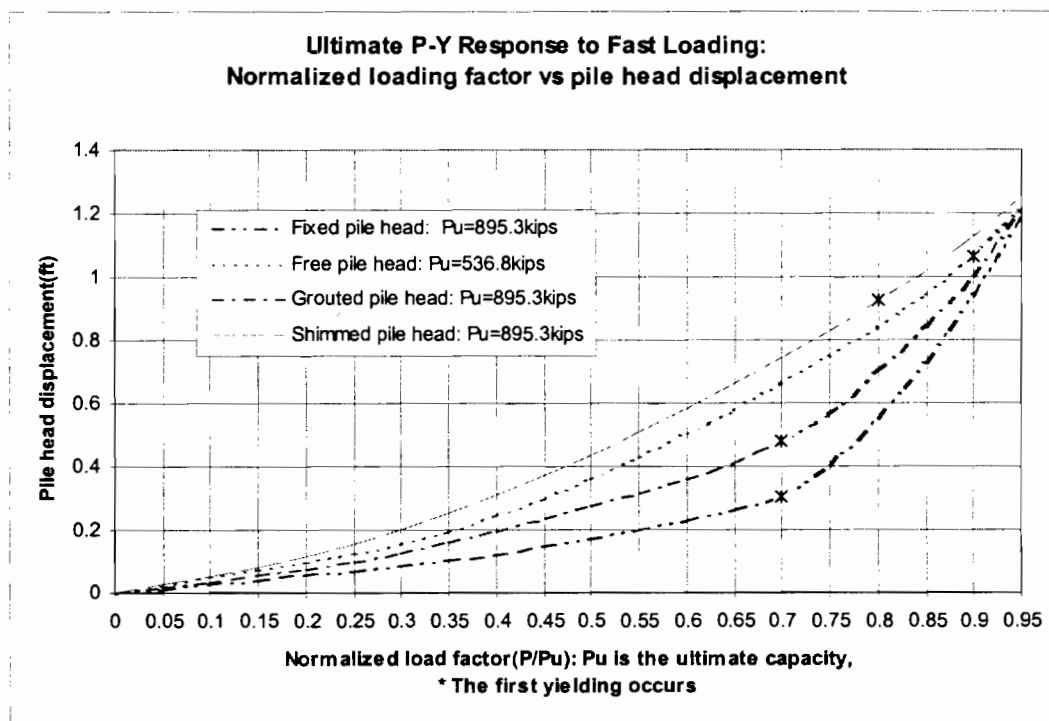
Figure 3.5 Displacement-loading relationship for fast loading

Ultimate Cyclic P-Y Response:
Normalized loading factor vs pile head displacement
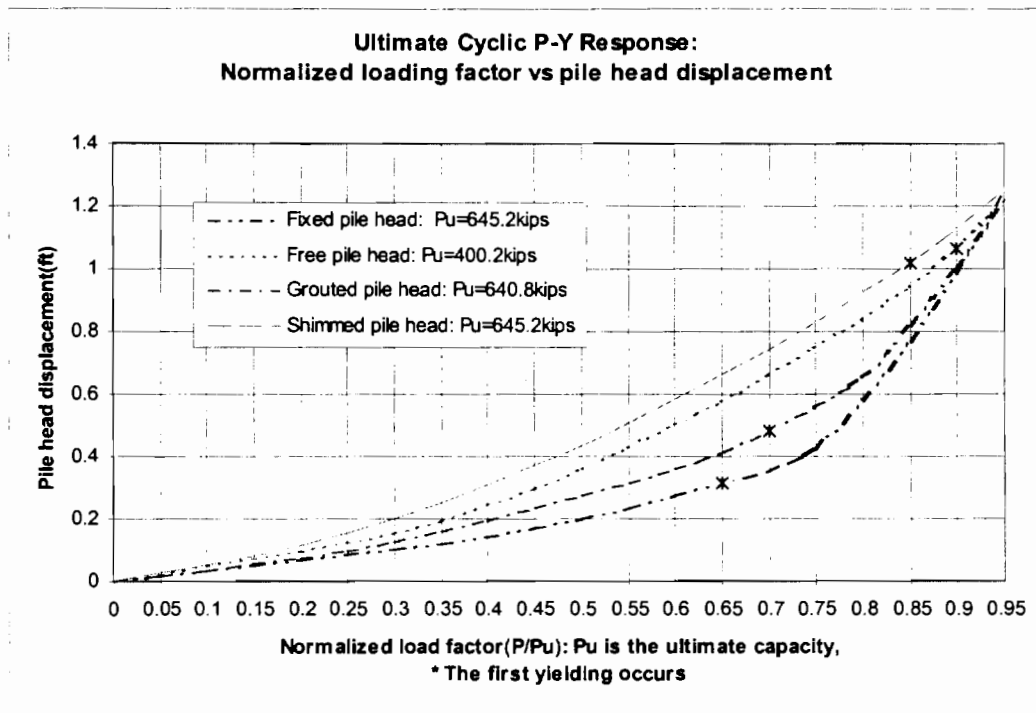
Figure 3.6 Displacement-loading relationship for cyclic loading

Typical Ultimate P-Y Response: Bending Moments at Pile
Stations(Fixed head and free head)
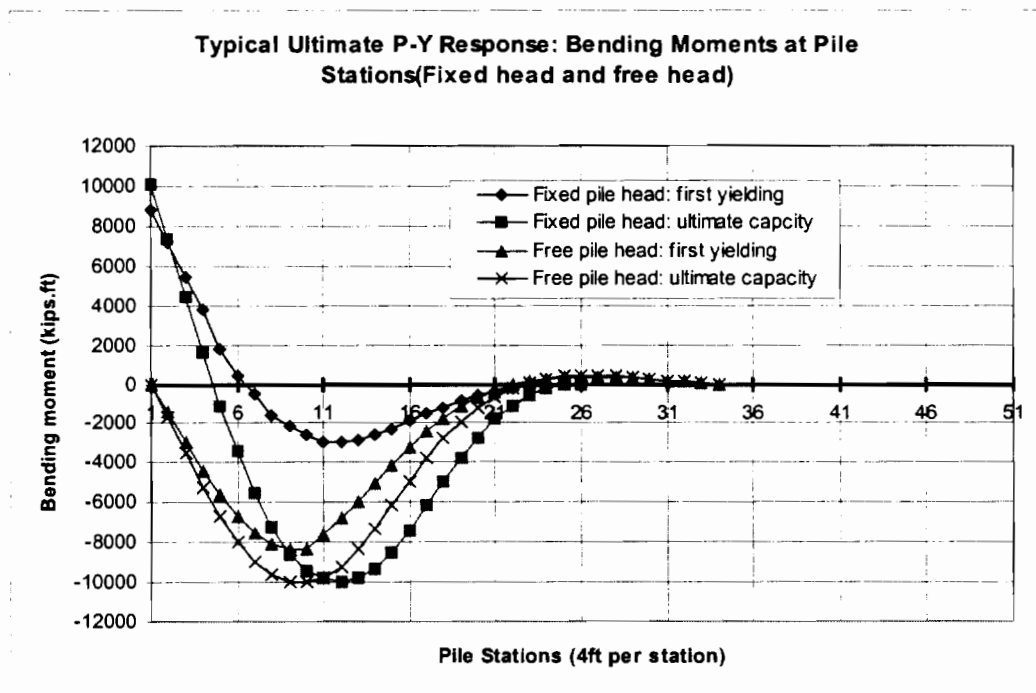
Figure 3.7   Bending moments at ultimate state(fixed and free pile head)
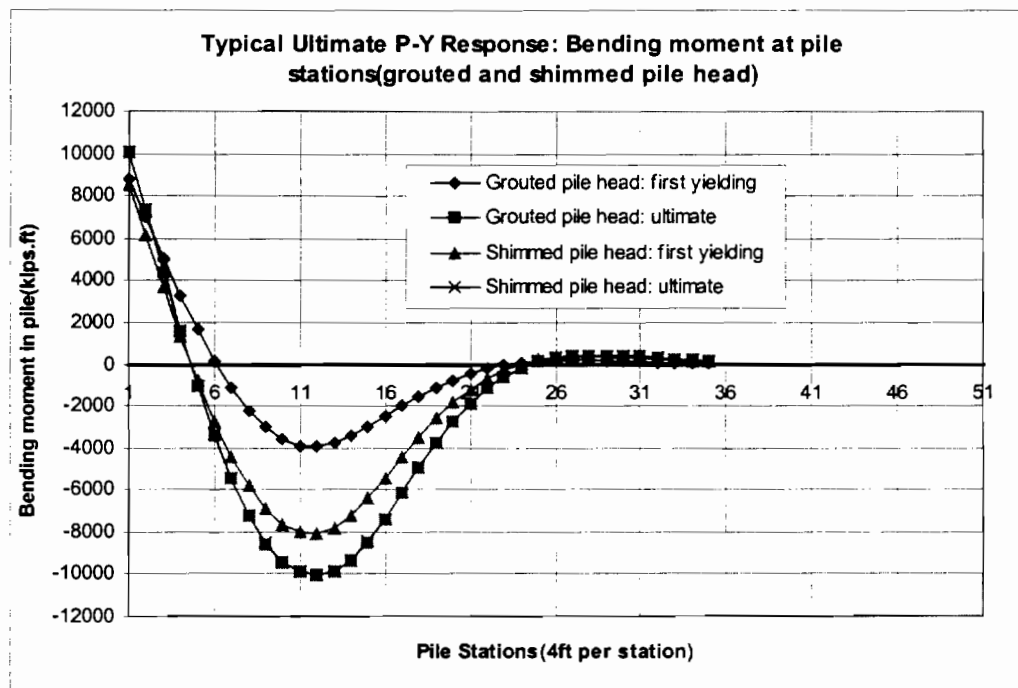
Figure 3.8 **Bending moments at the ultimate state(grouted and shimmed pile head)**

Chapter 4

Axial Pile Response

4.1   Set up of the analysis models

The analysis of the axial response of a single pile has the same framework as that of the lateral response. Drain3D and ULSLEA are used to evaluate the capacities of the pile-soil system. ULSLEA calculates the static ultimate axial capacity of the pile-soil system. Drain3D calculates the static and dynamic response of the pile-soil system.

Unlike the lateral response of the pile that has three major failure modes, the axial response of the pile-soil system is mainly determined by the soil resistance. It has only one major failure mode, i.e., failure of the soil resistance. The platform pile itself under normal axial loading very seldom reach the steel plastic range, thus never buckle or collapse due to axial loading. It is the failure of the soils that causes the excessive displacement of pile head, thus causes the failure of the whole pile-soil system.

4.1.1   Pile and soil properties

The pile and soil properties are the same as those in the lateral analysis. The decomposition process of the discrete pile-soil Winkler model keeps the same. The positions of the nodes and the lengths of the pile segments are not changed. As the axial loading is transferred from the jacket, the restrain at the pile is not a factor in consideration, unlike what was done in the lateral analysis. The basic soil profile is the same as that in the lateral analysis. Based on this backbone profile, the soil profile for the case of fast loading is modified. As the axial pile response is more sensitive to the loading rate effect than the lateral response, special care is taken to warrant this effect is reflected correctly in the modified t-z and q-z curves. This approach will be detailed in

section 4.3. As to the construction of the t-z and q-z curves, this study follows the API guideline, with a little modification. The construction process is detailed as follows:

T-Z curve

The unit ultimate friction for each layer of soils can be calculated using the formulae documented in section 2.3.3. The displacement (z_{max}) at which the ultimate friction capacity is mobilized is a function of soil stress-strain behavior, stress history, pipe installation method, pile load sequence and other factors. In this study, z_{max} is taken to be 0.01D, according to the recommendation of the guideline. The shapes of the t-z curves at displacements greater than z_{max} as shown in Figure 4.1 are carefully considered. There is no definite data available about the values of the residual adhesion ratio t_{res}/t_{max} in the Bay of Campeche. Also this parameter involves large uncertainties for soils in field. So two cases are studied, one with the displacement softening after the peak friction is mobilized, the other without displacement softening. Usually, the value of t_{res}/t_{max} can range from 0.70 to 0.90. The mean value 0.80 is chosen to use in the case of softening. This is regarded as the lower bound of the unit ultimate side friction. The case without displacement softening is regarded as the upper bound of the unit ultimate side friction. The values of z/D and t/t_{max} used in this study is listed in Table 4.1. The shape of the t-z curve is shown in Fig. 4.1.
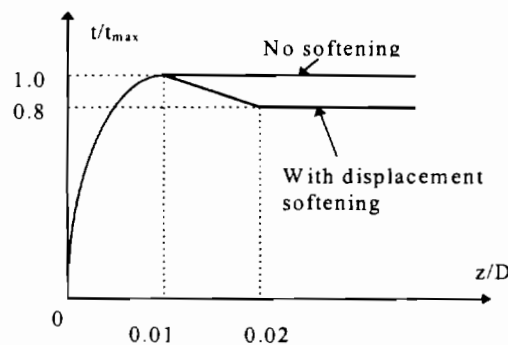
Fig. 4.1   t-z curves

Table 4.1 Coordinates in t-z curves

z/D	t/t_{max}
.0016	0.30
.0031	0.50
.0057	0.75
.0080	0.90
.0100	1.00
.0200	0.80(or 1.00)
∞	0.80(or 1.00)

where:

z   = local pile deflection, in. (mm)

D   = pile diameter, in. (Mm)

t   = mobilized soil pile adhesion, lb/ft^2 (kPa)

t_{max}= maximum soil pile adhesion or unit skin fraction capacity computed according to the API method described in Section 2.3.3, lb/ft^2 (kPa)

Q-Z Curve

The end bearing or tip load capacity Q_p can determined by equations described in Sections 2.3.3: $q=9*S_u$, S_u is the undrained shear strength. However, relatively large pile tip movements are required to mobilize the full end bearing resistance. A pile tip displacement up to 10 percent of the pile diameter may be required for full mobilization in clay soils. And compared with the side friction capacity, the ultimate bearing capacity is relatively small. The values of Q/Q_p and z/D are listed in Table 4.2. The shape of the q-z curve is shown in Fig. 4.2.

Table 4.2 Coordinates on the q-z curve

z/D	Q/Q_p
.002	0.25
.013	0.50
.042	0.75
.073	0.90
.100	1.00
∞	1.00
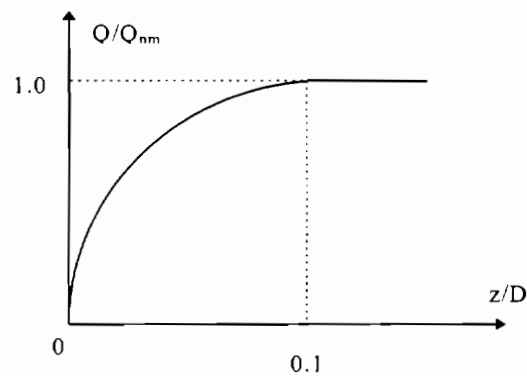
Fig 4.2 q-z curve

where:

z = Axial tip deflection, in. (mm)

D = pile diameter, in. (mm)

Q = mobilized end bearing, lb (KN)

Q_p = total end bearing, lb (KN), computed according to Section 2.3.3

4.1.2 Drain3D and ULSLEA models

Similar to the description in chapter 3, the Drain3D axial pile response model is a completely new one. The idea is to simulate the response of pile-soil system to loading by

an equivalent "solid" structure, i.e., a truss frame consists of steel column and soil supporting beam. The elements used in this Drain3D model are of type 1, type 4, and type 15. An illustration of such a truss frame is shown in Fig. 4.3. The details of the node connections and sub-element configurations are also shown in Fig. 3.2. Note that the axial soil beams can be actually regarded as being plugged in the steel pile. They are connected at pile nodes. The loading is allocated to pile and soil beams at these nodes. Since there are significant displacement softening for the axial response, the "rigid bars" are also added to each soil beams to prevent them from buckling before the ultimate soil friction capacity is mobilized. The soil beams simulating the t-z springs are 2 feet long. This length is chosen so that the largest strain occuring in the bar is less than 10% when it yields or reach the residual resistance. For the same reason, the soil beam simulating the q-z spring has a length of 4 feet. Just as in the lateral analysis, the soil beams are assigned to have zero resistance to tension. There are a pair of such soil beams with opposite orientations at each pile, one resisting the compression loading, the other resisting the tension loading.

The ULSLEA can only calculate the static ultimate capacity of the pile-soil system. It assumes a rigid pile. It also assumes that the maximum end bearing and side friction are mobilized at the same time. These assumptions greatly simplify the approach, but meanwhile, does not loss control of the major factors influencing the axial ultimate capacity. ULSLEA can not provide the information about the pile head displacement. The calculation method has been stated in section 2.3. The layered soil calculation is used. This method will be coded into ULSLEA as one of the phase IV research works. The total pile-soil system capacity is obtained by integration of the unit friction along the pile length. The results of ULSLEA are detailed in the following sections.

4.2   Axial response of a pile to the static loading

The axial response of the pile is calculated by Drain3D model. The pile head displacement-axial loading relationship is obtained and plotted as a graph. The prediction of axial ultimate capacity by different calculation method is listed in a table for comparisons.

4.2.1   Ultimate capacity predicted by DRAIN3D

For static loading, two cases are studied by Drain3D model. The first analysis considers the displacement softening after the peak friction resistance. The residual friction resistance is 80% of the peak value. The second one does not consider this softening. The two cases define a possible range of the static axial ultimate capacity. The capacity obtained by the first case is the lower bound. The ultimate capacity of the first case is around 80% of the second case. The second one is the upper bound. The results are listed in Table 4.3. The displacement-loading relationship is also obtained. This relationship is plotted in Fig. 4.4. It can be easily seen that the major portion of the axial capacity is contributed to side friction resistance. The end bearing is not very important. After the failure has occurred in all the t-z springs, The loading is transferred to the q-z springs. And the displacement increases drastically. For the pile-soil system with this configuration, there exists a maximum value for pile head displacement. Considering the fact that the end bearing q-z springs will fail as the pile tip displacement exceeds $0.1D=0.4$ft, the maximum pile head displacement is around 0.45ft.

4.2.2   Correlation with ULSLEA and API guidelines

The static ultimate axial capacity can be calculated by ULSLEA program. An estimation of this capacity can also be made following the API guidelines. The calculation methods have been detailed in section 2.3.3.

The comparisons of all these results are listed in Table 4.3. All the calculated capacities are pretty close. A good agreement between different calculation methods is achieved.

Table 4.3 Predictions of axial capacities

Axial capacities of a single pile (Calculated by DRAIN3D, ULSLEA and API Guideline)		
	Axial ultimate Capacity(kips)	
Calculation Methods	Static	Quick
Drain3D without displacement softening	3787	6430
Drain3D with displacement softening	3109	5601
ULSLEA(layered soils)	3103	4655
API calculation method	3390	non

One thing shall be made clear is that the ULSLEA result is obtained by assign maximum friction factors in Table 2.1. The capacity in Table 4.3 is possible maximum that can be predicted by ULSLEA. But the ULSLEA capacity value is still the smallest one. So it seems that ULSLEA under-estimated the axial ultimate pile capacity. The reason can be traced to the method of determining the side friction factor. In ULSLEA, the friction factor is a function of the average undrained shear strength (Table 2.1). While the API guideline takes an effective overburden pressure approach which is better in predicting the friction resistance (Tang, 1988). Drain3D also takes this way to predict the ultimate capacity. Anyway, the ULSLEA results are conservative, and tend to be on the safe side if it's predicted capacities are used in practical design.

4.3   Axial response of a pile to the dynamic loading

Two dynamic responses are studied: responses to the fast loading and to the cyclic loading. The fast loading increases the strength and stiffness of the soils thus increases

the ultimate capacity of the pile-soil system. The cyclic loading just do the opposite things.

Sully(1994) defined an approach to estimate the effective axial dynamic load carrying capacity based on the static axial capacity:

$$R_d = R_s \bullet \beta_c \bullet \beta_r \qquad (4.1)$$

Where R_s is the static capacity; R_d is the dynamic capacity; β_c reflects the cyclic loading effect; and β_r reflects the loading rate effect. The dynamic analysis in this study is trying to find the characteristics of β_c and β_r.

4.3.1   Fast loading

For fast loading, the loading rate effect is obvious. There are presently two ways to reflect these kinds of effects. The first is incorporate dynamic effects into the *t-z* and *q-z* characterizations. This was an implicit way to incorporate the effects. The second way was to apply a velocity-dependent strain-rate correction to the static backbone *t-z* and *q-z* curves.

Using the parameter β_r is the second approach. β_r is larger than 1 for fast loading. The dynamic capacity for fast loading is larger than the static capacity. For normally consolidated, moderate plasticity clays, r=0.10 to 0.20. The study of the available laboratory test data on the Bay of Campeche cohesive soils indicates that the r value for the soils under study can be taken as 0.15. If the static loading rate of the pile is 24 hours and the average loading rate from storm waves is 3 seconds, The β_r value turns out to be 1.67.

The Drain3D take the similar approach. The static backbone t-z and q-z curves were modified by a factor of 1.5, just as how the p-y curves were modified in lateral analysis. The soil beams' properties are modified according to the new t-z and q-z curves. The "concrete" strain-stress relationships for the material of the soil beams are then corrected for the fast loading. The results of the time-history of the pile-soil system response are plotted in Fig. 4.4. Compared with the static response, the ultimate capacity for fast loading is about 1.7-1.8 times the static ultimate capacity, which is comparable with the β_r value. The increase in ultimate capacity is a little higher than the increase of resistance in t-z and q-z curves. This is due to the viscous damping at the high loading rates.

The above results are quite reasonable. The loading effects is due to the viscous behavior of the soils, that is, their strength depends upon the rate at which they are sheared. This behavior extends to the observed capacity of piles installed in clays. The ultimate capacity of pile in clays reportedly increases between 5 and 20 percent for each order of magnitude increase in loading rate. In the absence of soil strength degradation due to load cycling, axial capacities of piles in clay that are loaded by storm waves could be 30 to 80 percent greater than capacities calculated using static design procedures (Bea, 1980). The results of this study provide more support to this argument.

4.3.2 Cyclic loading

The cyclic loading analysis needs the soil supporting beams exhibit strength degradation behavior. Element type 15 in Drain3D does have a degradation mechanism in element stiffness and strength. However, a cyclic model by this way doesn't work well in simulating the pile-soil response. The degradation mechanism is originally designed to reflect the "pull-out" bar degradation in the re-enforced concrete. The degradation is concentrated at the connection between elements. The degradation process is a function of the element's accumulated plastic displacement. It does not fit the soil

degradation process defined by Matlock(1978). By now, the Drain3D model has not been developed to be a valid analysis tool with respect to the cyclic axial loading yet. A new, more specific element is needed to simulate the soil degradation. This work can be done in the future if needed. Although the model is not good enough to do the detailed analysis, reviewing of the related research can lead to some valuable general comments about the axial cyclic response problem.

Existing experimental and analytical programs show that the cyclic pile problem is complex. The recent research efforts have identified several factors that influence cyclic axial pile performance, including:

- static capacity;
- the nature of the cycling, including the magnitude of the sustained and cyclic load components and whether the pile is cycled using load control or displacement control;
- viscous soil behavior(rate effects);
- displacement softening behavior of soil resistance-vs.-pile displacement (t-z) relations;
- the stiffness of the pile relative to the soil; and
- the number of cycles applied at each given load level

Each of these factors is important, and should be considered when assessing the likely behavior of a pile under storm loading.

Based on the research works of Bea(1992), and Clukey(1990), cyclic axial pile response has it's unique patterns. The cyclic loading effect in equation (4.1) can be estimated by:

$$\beta_c = 1 - \Delta(1-\delta) \qquad\qquad (4.2)$$

54

where Δ = the ratio of percentage change in soil strength to percentage change in soil stiffness; and δ = the degradation index:

$$\delta = N^{\cdot} = \frac{Gn}{G_{\cdot}}$$

where N = the number of cycles of peak strain (fully reversing harmonic straining); t = the degradation parameter (function of peak strain and soil); and G = the shear modulus at $N = 1$ and n cycles. β_c is the ratio of the capacity of the pile after design cyclic loading to the static capacity. The cyclic-loading factor is generally less than unity and can be based on results of laboratory cyclic or model and prototype pile tests. For a moderate-plasticity, normally consolidated clay, estimates of $\Delta = 0.5$, $t = 0.1$ (0.1% cyclic shear strain), $N = 10$ (equivalent number of cycles of design loading) results in $\beta c = 0.9$.

The cyclic degradation mechanism for axial response can be formulated in a similar way as that used in the SPASM lateral analysis (Bea, 1992; Matlock, 1980):

For small levels of strain, the degradation index is reasonably linearly related to the number of cycles of the strain. For high levels of strain (greater than 1-2%), which is the case for near-field soils, the degradation factor was used with a specified residual capacity. The shaft resistance at cycle N, t_n, was computed as:

$$t_{\scriptscriptstyle N} = \delta\left(t_{\scriptscriptstyle N} - t_{\scriptscriptstyle res}\right) + t_{\scriptscriptstyle res}$$

where t_{res} = the residual level of capacity (e. g. $t_{res} \approx t$ remolded). This is a modified from of the model proposed by Matlock and Foo (1979) in which:

$$\delta = (1 - \lambda)$$

where λ = a model parameter that is used to fit measured data from soil tests or model pile tests. The minimum degradation parameter, δ_{min} was taken to be the reciprocal of the clay sensitivity (δ_{min} = 0.33 - 0.25). This degradation mechanism should be incorporated into a new Drain3D model to accurately simulate the soil behavior under cyclic loading.

The degree to which cyclic loading degrades static skin friction depends upon the relative magnitudes of the sustained and cyclic load components and on whether the cycling is with respect to pile head loads or to pilehead displacements (load or displacement control). With all else being equal, damage to pile performance generally decreases either as:

- the magnitude of cyclic loads, as a fraction of ultimate pile capacity, decreases, or
- the amplitude of imposed cyclic displacements decreases.

Strictly speaking, the local nature of the cycling and the resulting damage must be evaluated at each point along the pile. This is because pile-soil relative stiffness effects reduce the correspondence between cyclic pilehead loads and the resulting soil stresses. For example, stress reversals can occur in the soil near the tops of long piles that are subjected to wholly compressive or tensile cyclic loads.

One-way cycling in clays without local soil shear stress reversals normally causes little reduction in peak skin friction; damage from such cycling is manifested predominately in accumulated displacements. Piles in firm to hard clays reportedly have resisted several hundred one-way load cycles when the peak pile load was less than 0.75 - 0.80 static capacity.

Two-way cycling, i.e., subjecting the soil around a pile to both positive and negative shearing stresses, is much more damaging than one-way cycling. Failure due to increased displacements reportedly has occurred during symmetric two-way loading tests of stiff piles. Large amplitude two-way displacement-controlled cycling can be the most damaging of all. It was found in one case the skin friction is reduced to about thirty percent of the undegraded static skin friction. The skin friction that is lost during two-way cycling in non-strain-softening clays generally is recoverable by soil reconsolidation aft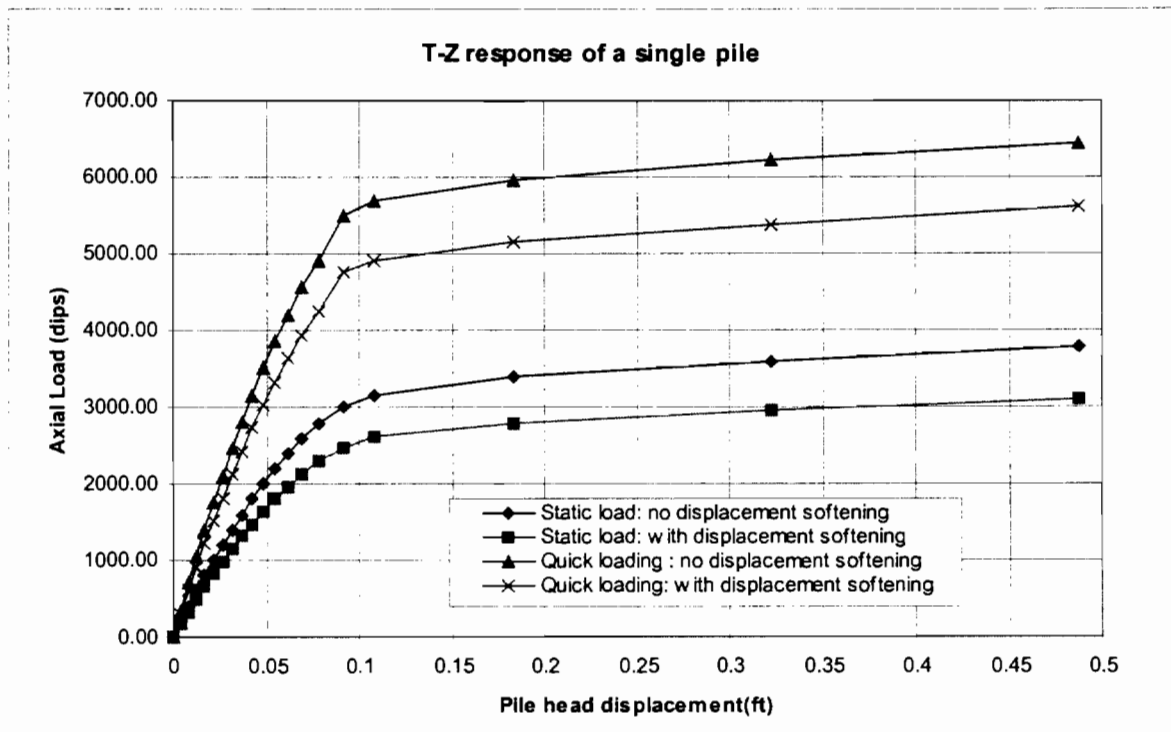er cycling. This suggests that frictional resistance that is lost in such soils during a major storm probably can be substantially reestablished before another major storm occurs. However, some results in clays with displacement-softening t-z behavior show incomplete strength regain after cycling. It cam be inferred from this collective experience that a foundation's survivability through multiple design storm perhaps does not need to be investigated unless the supporting clay exhibits strain softening behavior.

The stiffness of a pile relative to the soil in which it is embedded can influence the pile's cyclic performance substantially. Considering the following special case, an infinitely stiff pile that is subjected to one-way cyclic pile head loads will induce relatively undamaging one-way stress cycling along its entire length. On the contrary, a pile with a finite stiffness that is loaded with one-way cycles can subject the soil along a substantial portion of its length to damaging two-way cycles. The second pile will have a lower static capacity after cycling than will the first pile.

One thing shall be emphasized that the foregoing comments may not be regarded as general. They are appropriate for the particular pile, soil, and loading conditions evaluated in the analyses. More comprehensive analyses of the dynamic response characteristics of offshore piles embedded in marine soils and subjected to realistic characterizations of marine-structure pile loadings ate needed to permit development of general engineering guidelines for consideration of dynamic cyclic-loading effects on piles.

Axial load: T

Mudline

Two nodes with actually the same coordinates

Artificial rigid bar

Pile head

Artificial nodes rotationally fixed

Non-linear supporting bar simulating the t-z springs: no resistance to tension force.

Two compression supporting non-linear bars at each nodes, the force-displacement relationships of these bars are determined by t-z curves. Two cases considered: with and without displacement softening

Non-linear steel pile

Node in the pile model

Fixed boundary

2.0ft

0.1ft

Same coordinate nodes

4.0ft

Non-linear supporting bar simulating q-z springs with the force-displacement shown at the left

t/t₊ t-z curve with softening

1.0

0.75

0   0.01   0.02   z/D

t/t₊ t-z curve without softenting

1.0

0   0.01   z/D

q/q₊ q-z curve at pile tip

1.0

0   0.1   z/D

D is the pile diameter

Fig 4.3   Equivalent truss frame simulating the axial response of the pile-soil system

T-Z response of a single pile

Axial Load (dips)

7000.00
6000.00
5000.00
4000.00
3000.00
2000.00
1000.00
0.00

Pile head displacement(ft)

0   0.05   0.1   0.15   0.2   0.25   0.3   0.35   0.4   0.45   0.5

Legend:
- ◆ Static load: no displacement softening
- ■ Static load: with displacement softening
- ▲ Quick loading : no displacement softening
- ✕ Quick loading: with displacement softening

Fig 4.4 Pile head displacement - axial load relationship

for static and fast loading

Chapter 5

Summary and Conclusion

5.1   Summary

A systematic analysis of the offshore pile foundation response and its ultimate characteristics has been finished. There are mainly three computers codes used in the analysis. Drain3D, SPASM and ULSLEA. Drain3D model is a new pile analysis tool developed by Marine and Management Technology Group in the Department of Civil and Environmental Engineering, University of California at Berkeley. It extends the analysis scope to non-linear steel pile and non-linear-hysteretic soil supporting. It can handle both lateral and axial response of the single pile. It can calculate the dynamic response of the pile by a time-history approach, either displacement control or load control. The SPASM is a specific pile analysis tool for lateral loading. It assumes an elastic pile. It can couple the complicated interaction between the linear pile and the hysteretic soil springs. ULSLEA is a simplified ultimate state analysis tool. It can give very good estimation of the lateral and axial ultimate capacity of a single pile, although it has a very simple approach.

Using these analysis tools, lateral loading and axial loading analyses are performed.

The lateral analysis includes a set of standard cases. The loading patterns, soil characteristics, and pile configuration are systematically changed to reflect the effects of cyclic loading, fast loading and the ultimate state properties for different combination of all these variables. It is intended to capture the impacts on the pile response and ultimate capacity by the natural variation. The results from different analysis tools are compared. Valuable conclusions about the response and ultimate states of the laterally loaded piles are obtained.

The axial analysis takes the similar framework as the lateral analysis. The static and fast loading cases are successfully studied. The loading rate effect has been identified. The validity of the simplified ULSLEA program has be proved. The possible range of the axial ultimate capacity is defined based on the variation in the residual resistance after the peak value. A cyclic axial model has been built. Although the simulation of the pile-soil response is not as good as expected, a study of the features of the cyclic degradation, cyclic loading pattern, relative pile stiffness, etc, leads to some general comments on the cyclic axial pile response problem.

Based on the calculation results, simplified approach such as ULSLEA and the more complex, more realistic models such as SPASM and Drain3D are compared with respect to their efficiency, accuracy. Correlation between these methods proves the validity and accuracy of the ULSLEA program and provides some information about the bias developed from the program compared with API guidelines.

5.2   Conclusions

From the analysis results, some useful conclusions can be drawn:

- For lateral loaded pile, three failure modes exist: excessive pile head displacement; permanent damage to the pile; and ultimate collapse.
- For the pile configuration under study, pile rigidity is not an important factor influencing the ultimate capacity, all shimmed, grouted, and fixed pile heads have the similar lateral ultimate capacity. Free pile head is an exception.
- For the pile configuration under study, pile rigidity is an important factor influence the first yielding capacity, and the reserve strength of the pile. Stiff pile head is prune to suffer permanent damage but has large reserve strength. Flexible pile head is not easy to yield, but has little robustness.

- For the pile configuration under study, there exists a maximum later pile head displacement. The pile is doomed to fail if the pile head displacement exceeds this value.
- The cyclic degradation will cause 20-30% loss of static lateral capacities, both first yielding capacity and ultimate capacity.
- The loading rate effect will cause around 20% increase in lateral dynamic capacity with respect to the static capacity.
- For the pile-soil system under study, the axial loading rate effect increases the dynamic capacity by 70-80% with respect to the static axial capacity.
- The end bearing capacity is not as important as the side friction for the axially loaded piles. For the pile configuration under study, the maximum pile head displacement is a little larger than 10% of the pile diameter.
- The displacement softening occurring during the axial loading process decreases the ultimate axial capacity by around 20%.
- For the case of lateral loading, ULSLEA can give a very good estimation of the ultimate capacities no matter the pile heads are fixed, shimmed or grouted.
- For the case of axial loading, ULSLEA capture the lower bound of the ultimate capacity, thus is conservative in practice.
- In practice, ULSLEA has good validity in predicting the ultimate capacities of the platforms' pile foundations.

In one word, ULSLEA is a valid and powerful analysis tool in the evaluation and requalification of the offshore platforms. This study has proved its advantage. Although there are a lot of assumptions made in it's simplification process, the final output of this simplified program is still accurate enough compared with the complicated and time-consuming methods. ULSLEA program has a very low cost-benefit ratio.

References

Aaghaakouchak, A. A., Asgaroan, B.(1996), "Dynamic Characteristics of a Jacket Type Offshore Structure Considering Non-Linear Behavior of Pile Foundations", 1996 OMAE--Volume 1--Part A, *Offshore Technology*, ASME 1996.

Aggarwal, R. K., Litton, R. W., Cornell, C. A., Tang, W. H., Chen, J. H., Muff, J. D., "Development of Pile Foundation Bias Factors Using Observed Behavior of Platform During Hurricane Andrew", *Proceedings of Offshore Technology Conference*, OTC 8078.

American Petroleum Institute, API. *Recommended Practice for Planning, Designing and Constructing Fixed Offshore Platforms*. API Recommended Practice 2A (RP 2A)-LRFD. 20, August, 1993, Dallas, Texas.

Barltrop, N. D. P., and Adams A. J., *Dynamics of Fixed Marine Structures*, Third Edition (1991), The Marine Technology Directorate Limited.

Bea, R. G., *Hurricane and Earthquake Criteria for Design and Requalification of Platforms in the Bay of Campeche,* report to PEMEX, IMP, and Brown and Root International, Inc., Marine Technology and Management Group, University of California at Berkeley, November. 1997.

Bea, R.G., Audibert, J.M.E., and Dover, A. R., "Dynamic Response of Laterally and Axially loaded Piles", Proceedings, 12th Annual Offshore Technology Conference, Paper OTC 3749, Houston (May, 1980) Vol. II, 129-139

Bea, R. G., "Analysis of Tension leg Platform Pile Foundations for Dynamic Loading", *Geotechnical News--Newsletter of the North American Geotechnical Community,* Volume 10, Number 2, June, 1992.

Bea, R. G., "Dynamic Response of Marine Foundation", *Proceedings of Ocean Structural Dynamics Symposium*, Oregon State University, Corvallis, Oregon, September, 1984.

Bea, R. G.(1994), *Evaluation of the Reliability of a Conventional Platform Installed in South Pass Block 47.*

Bea, R. G. , Litton, R. W. and Chang, J. Y.(1984), "A Specialized Design and Research Tool for the Modeling of Near-Field Pile-Soil Interactions", *Proceedings of Offshore Technology Conference*, OTC 4806.

Bea, R. G., "Pile Capacity for Axial Cyclic Loading", *Journal of Geotechnical Engineering*, Vol. 118, No. 1, January, 1992.

Bea, R. G., *Risk Based Hurricane and Earthquake Criteria for Design and Requalification of Platforms in the Bay of Campeche*. Report to Petroleo Mexicanos, September 1997.

Budkowaka, B. B. and E. Cean (1996), "Comparative Sensitivity Analysis of Laterally Loaded Piles", *Proceedings of the Sixth-International Offshore and Polar Engineering Conference*, Los Angeles, May, 1996.

Dunnavant, T. W., Clay, E. C, Murff, J. D.(1990), "Effects of Cyclic Loading and Pile Flexibilities in Clay", *Proceedings of Offshore Technology Conference*, OTC 6378.

Earth Mechanics, Inc., "Dynamic Soil-Pile Interaction Analysis, Group Va Sites Borings YAXILTUM-101, YAXILTUM-1, IB-102, CEEH-101, Moan-1, Tabay-1 and Kayab-1, Bay of Campeche, Mexico", Report to Fugro-McClelland Marine Geosciences, Inc, May, 1994.

Emrich, W. J. , "Performance Study of Sampler for Deep-Penetration Marine Borings", Sampling of Soil and Rock.

Folse, M. D. "Reliability Analysis for Laterally Loaded Piles", *Journal of Structural Engineering*, ASCE .

Jin, Z. and Bea, R. G., *Dynamic Response of a Single Pile to the Lateral Loading*, report to PEMEX, IMP, and Brown and Root International, Inc., Marine Technology and Management Group, University of California at Berkeley, August, 1997.

Jin, Z. and Bea, R. G., *Dynamic Lateral and Axial Loading Capacities of Piles in the Bay of Campeche*, report to PEMEX, IMP, and Brown and Root International, Inc., Marine Technology and Management Group, University of California at Berkeley, December, 1997.

Kraft, L. M., Cox, W. R., Verner, E. A., "Pile Load Tests: Cyclic Loads and Varying Load Rates", Journal of the *Geotechnical Engineering Division, Proceedings of the American Society of Civil Engineers*, ASCE, Vol.107, No. GT1, January, 1981.

Kraft, L. M., Forht, J. A., Amerasinghe, S.F., "Friction Capacity of Pile Driven into Clay", *Journal of the Geotechnical Engineering Division, Proceedings of the American Sociey of Civil Engineers*, ASCE, Vol.107, No. GT11, November, 1981.

Lok, T. M. and Pestana, J. M.(1996), "Numerical Modeling of the Seismic Response of Single Piles in a Soft Clay Deposit".

Matlock, H. (1970), "Correlation for Design of Laterally Loaded Piles in Soft Clay", *Proceedings of Offshore Technology Conference*, OTC 1204.

Matlock, H., Foo, S. H. C., "Axial analysis of piles using a hysteretic and degrading soil model", *Numerical methods in Offshore Piling* (1980).

Matlock, H., Foo, S. H. C., Tsai, C. F.(1979), *SPASM 8 , A Dynamic Beam-Column Program for Seismic Pile Analysis With Support Motion.*

Matlock, H. , Ingram, W. B. , Kelley, A. E. and Bogard, D(1980), "Field Tests of the Lateral-Load Behavior of Pile Groups in Soft Clay", *Proceedings of 12-th Offshore Technology Conference*, OTC 3871.

Matlock, H. and Foo, S. H. C. (1978), "Simulation of Lateral Pile Behavior Under Earthquake Motion", A Report to Chevron oil Field Research Company, La Habra, California, on Research Performed at the University of Texas at Austin, Department of Civil Engineering.

Meyer, P. L., Holmquist, D. V. And Matlock, H., "Computer Predictions for Axially-loaded Piles with Nonlinear Supports", *Proceedings of Offshore Technology Conference*(May, 1975), OTC 2186.

McClelland, B. and Focht, Jr. J. A. (1958), "Soil Modulus of Laterally Loaded Piles", Transactions, ASCE, Vol. 123, Paper No. 2954.

Mortazavi, M., and Bea, R.G., "Screening Methodologies for use in platform assessments and requalifications", final project report, Marine Technology and Management group, Dept. of Civil Engineering, University of California, Berkeley, Jan., 1996.

Prakash, V., Powell, G. H., Campbell, S., Drain-2DX Base Program Description and User Guide. Version 1.10, November 1993.

Prakash, V., Powell, G. H., Campbell, S., Inelastic Truss Bar Element (Type 01) For Drain-2DX (Element Description and User Guide), Version 1.10, December 1993.

Powell, G. H., Campbell, S., Drain-3DX Element Description and User Guide For Element Type 01, Type 04, Type 05, Type08, Type09, Type15,and Type17, Version 1.10.

Prakash, V., Powell, G. H., Campbell, S., Drain-3DX Base Program Description and User Guide, Version 1.10.

Poulos, H. G.(1981), "Cyclic Axial Response of Single Pile", Journal of the Geotechnical Engineering Division, *Proceedings of the American Society of Civil Engineers*, ASCE, Vol.107,No. GT1.

Quiros, G. W. , Asce, A. M. , Young, A. G., Pelletier, J. H. , Chan, J. H-C, "Shear Strength Interpretation For Gulf of Mexico Clays", *Offshore Engineering Practice*,

Reese, L. C. ,Cox, W. R.and Koop, F. D.(1974) , "Analysis of Laterally Loaded Piles in Sand", *Proceedings of 6-th Annual Offshore Technology Conference*, OTC 2080.

Ruiz, S. E., "Reliability Index for Offshore Subjected to Bending", *Structural Safety*, Vol. 2, 1984.

Ruiz, S. E., "Non-Dimensional Probabilistic Coefficients for Laterally Loaded Piles", *Structural Safety*, Vol. 4,1986.

Ruiz, S. E., "Uncertainty About p-y Curves for Piles in Soft Clay", *Journal of Geotechnical Engineering*, ASCE, Vol. 112, No. 6.

Singh, Gurdev, Lai, W. T. , Das, Braja, M.(1996), "Sensitivity of Probabilistic Pile Design to Various Uncertainties", *Proceedings of the Sixth-International Offshore and Polar Engineering Conference*, Los Angeles, May, 1996.

Shamsher Prakasher, Sanjeev Kumar(1996), "Analysis of Pile Supported Offshore Structures Under Wave Loading", *Proceedings of the Sixth-International Offshore and Polar Engineering Conference*, Los Angeles, May, 1996.

S. Narasimha Rao and V. G. S. T. Ramakrishna(1996), "Behavior of Laterally loaded Model Pile Group in Clay", *Proceedings of the Sixth-International Offshore and Polar Engineering Conference*, Los Angeles, May, 1996.

Stear D. James, "Screening Methodologies for Use in Platform Assessments and Requalifications", Project Progress Report 9, Report to Project Sponsors, UC Berkeley, October 31, 1997.

Sullivan, W. R. , Reese, L. C. and Fenske, C. W.(1980), "Unified Method for Analysis of Laterally Loaded Piles on Clay", *Numerical Methods in Offshore Piling*, Institution of Civil Engineering's, London, England.

Tang, W. H. (1988), "Offshore Axial Pile Design Reliability", Research Report for Project PRAC 86-298.

Tang, W., H and Gilbert, R., B.(1990), "Offshore Lateral Pile Design Reliability", Research Report to Project PRAC 87-29.

Valle-Molina, Celestino, *Modelado Del Comportamiento De Pilotes De Friccion Bajo Carga Axial Eststica y Ciclica.* Tesis Presentada a la Division de Estudios de Posgado de la, Facultad de Ingenieria de la Universidad Nacional Autonoma de Mexico, 1997.

Wang, S. , Kuter, B. L. , Jacob Chacko, M. and Wilson, D. W.(1996), "Nonlinear Seismic Soil-Structure Interaction".

Young, A. G., Quiros, G. W. and Ehlers, C. J.(1983), "Effects of Offshore Sampling and Testing on Undrained Soil Shear Strength", *Proceedings of Offshore Technology Conference.* OTC 4465.